PROPX: Definitions, Derivations, and Data Flow

Written By

C. Ross Harman
Department of Mechanical Engineering
Oregon State University

August, 1994

Table of Contents

1.0 Introduction 3
2.0 Propx Main Program 4
- 2.1 PROPX Data Files 4
- 2.2 Data Initializations 6
- 2.3 Tip Speed Ratio 6
- 2.4 Density and Viscosity 6
- 2.5 Tip Drag 7
- 2.6 Integration Loop 8
- 2.7 Thrust and Power Coefficients 10
- 2.8 Efficiencies 10

3.0 Subroutine Readfl 12
4.0 Subroutine Calc 15
- 4.1 Relative Inflow Angle 15
- 4.2 Angle of Attack 17
- 4.3 Cascade Effects 17
- 4.4 Aerodynamic Coefficients 18
- 4.5 Tip Loss Factor 18
- 4.6 Axial and Tangential Induction Factors 19
- 4.7 Momentum Equation Correction 26
- 4.8 Computational Instabilities 29
- 4.9 Final Calculations 30
- 4.10 The Effect of the Tangential Induction Factor 30

5.0 Airfoil Subroutines 33
- 5.1 NASA LS(1) Airfoil 33
- 5.2 NACA 23000 Airfoil 33

6.0 Subroutine Check 38
- 6.1 Derivation of Tip Frequency 38
- 6.2 Blade Static Tip Displacement 43
- 6.3 PROPX Implementation 44
- 6.4 Final Calculations 47

Bibliography 48
Appendix A: Propx Input File 49
- A.1 Input file format 49
- A.2 Explanation of Inputs 52

Appendix B: Propx Output File 54

1.0 Introduction

PROPX is a FORTRAN computer program that predicts horizontal axis wind turbine performance. Although not as sophisticated as some codes, it gives a good initial impression of performance with a minimal of required input data. PROPX accounts for effects such as: Prandtl tip losses, wake expansion effects, cascade effects, rotating wake effects, blade coning, gap corrections, generator losses, blade twist, and airfoil characteristics for variable thickness blade sections. The program also calculates the frequency and static tip displacement of the rotor blades for the first flatwise bending mode as a function of wind speed.

The core of the program uses a combined blade element/momentum theory approach to the determine force, torque, and power acting on the rotor blade as a function of wind speed. This theory is implemented with integration and iteration techniques limited in accuracy only by the incrementation the step size.

Input and output for PROPX are maintained in user friendly formats which allow for quick data analysis. Wind turbine characteristics are input into an approximately one page text format data file read directly by the main program. The output file prints turbine vital performance parameters with the option of an expanded output for more detailed analyses. Both the input and output files are accessible by almost any text editor or word processing program .

2.0 Propx Main Program

The primary function of the PROPX main program is to calculate the force, torque, and power generated by the wind turbine. These are calculated over a range of wind speeds by summing and incremental distances along the blade surface with a Simpson's Rule integration algorithm. The main program accomplishes this through a series of call series of call statements to smaller subroutines that calculate and return variables to the main program. The order in which these subroutines and their sub-subroutines are called is shown below.

Main Program
- Subroutine Readfl
  - Subroutine Readln
- Subroutine Titles
- Subroutine Search
- Subroutine Calc
  - Subroutine Super
    - Subroutine Nnaca
  - Subroutine Nacaxx
  - Subroutine Nasals
  - Subroutine Tiplos
  - Subroutine Calcap
- Subroutine Check
  - Subroutine Sear
  - Subroutine Shape
  - Subroutine Ccalc

The main program also serves to open data files, initialize variables, convert units, determine power losses, increment wind speed, and print output. The flow chart in Figure 4.1 illustrates the computational process of the main program.

2.1 PROPX Data Files

One of the first things PROPX does is to open the input file and create the output file. The input file contains description of the wind turbine characteristics that PROPX uses make calculations. This file is read by subroutine Readfl and its format further described in Appendix A.

The output file contains the performance data and the general operating conditions of PROPX. There is an option for a standard output or an expanded output format for this file, depending on the amount of information desired. A further description of the output file is provided in Appendix B.

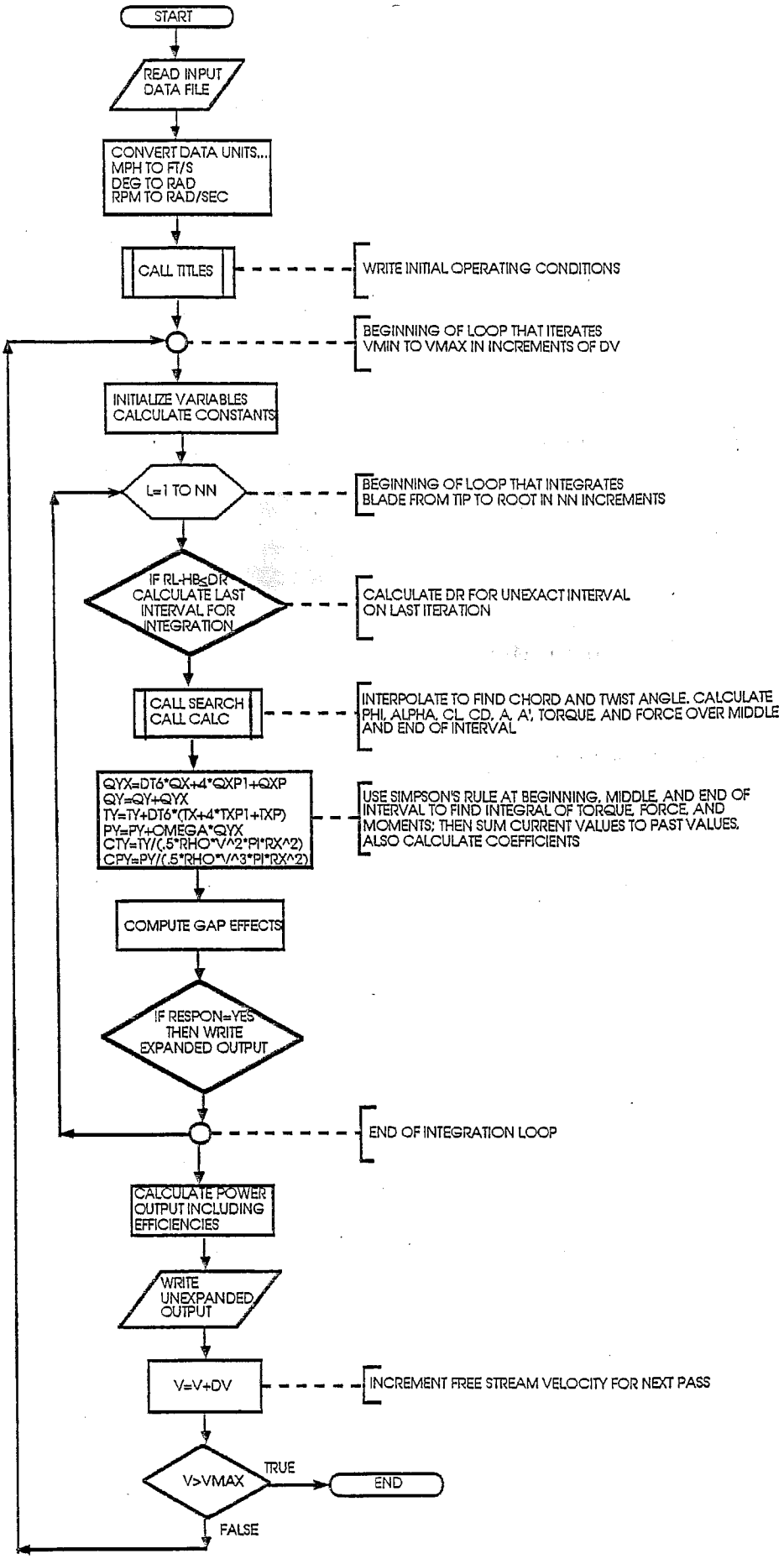

Figure 4.1. Flow Chart for PROPX Main Program.

2.2 Data Initializations

After PROPX opens and creates the necessary data files, it initializes the data read from the input file. The initialization sequence covers a broad range of basic calculations and variable assignments such as converting units, zeroing variables, and calculating initial operating conditions. Units that undergo conversion include: miles per hour to feet per second; degrees to radians; and rotations per minute (RPM) to radians per second. Initial quantities calculated include: tip speed ratio, density, viscosity, tip brake drag effects, and the blade incrementation. The formulation of these quantities is described below.

2.3 Tip Speed Ratio

The tip speed ratio is a basic, non-dimensionalized term used to describe the rotor speed. There are a number of deviations used throughout PROPX based on the tip speed ratio. These are defined as

$$X = \frac{R\Omega}{V} \equiv \text{Total tip speed ratio}$$

$$x = \frac{r\Omega}{V} \equiv \text{Local tip speed ratio}$$

$$X_L = \frac{R\Omega\cos\psi}{V} \equiv \text{Total tip speed ratio for a coned blade}$$

$$x_L = \frac{r\Omega\cos\psi}{V} \equiv \text{Local tip speed ratio for a coned blade}$$

Where

R = Blade tip radius

r= Blade local radius

ψ = blade coning angle

V = free stream velocity

2.4 Density and Viscosity

The density, ρ, is calculated with the universal gas equation commonly formulated as

$$\rho = \frac{P}{RT}$$

In PROPX this is modified in English units to be

$$\rho = \frac{2.08922P}{1714.87[T + 459.6]}$$

where

T = Ambient temperature in °F (from input file)

P = Ambient pressure in millibars (from input file)

ρ = Ambient density in slugs/ft^3

It is also necessary for PROPX to calculate viscosity when determining the Reynold's Number. Viscosity is a function of temperature can be determined from

$$\mu = \frac{bT^{\frac{3}{2}}}{S + T}$$

where S and b are constants

In PROPX this is modified for English units to be

$$\mu = \frac{2.26968 \times 10^{-8}(T + 459.7)^{\frac{3}{2}}}{T + 658.4}$$

where

μ = is the viscosity in slugs/(ft-s)

2.5 Tip Drag

The friction drag of the rotor tip is associated with the shear stresses of the air in the boundary layer as it passes over the surface. For the tip of a wind turbine it is assumed that the boundary layer is in the turbulent regime. The drag for such a flow can be estimated with [1]

$$D_{Tip} = \frac{1}{2}\rho W^2 cBC_f$$

where

$$C_f = \frac{.07}{Re_c^{.2}}$$

$$Re_c = \frac{\rho W c}{\mu}$$

c = Chord length of tip (ft)

W = Tip velocity (ft/sec)

B = Number of blades

PROPX also calculates the drag associated with tip brakes used to control the turbine and slow it when the winds becomes too powerful. This can be estimated from the equivalent flat plate area of frontal area in contact with the surface in the flow. This is given by

$$D = \frac{1}{2}\rho W^2 B f$$

2.6 Integration Loop

Once PROPX makes all initial calculations, it begins the integration loop. The turbine blade is integrated from tip to hub with a three point integration algorithm known as Simpson's Rule. This method has a forth order accuracy and is favored over the popular Trapezoidal rule, which only has second order accuracy. With the increased accuracy, however, comes a slightly longer computational time, but almost negligible with today's high speed computers.

The Simpson's Rule method uses three points to form a quadratic curve fit over the interval from a to b shown in Figure 2.2 The three points that make up the interval at the beginning, middle, and end.

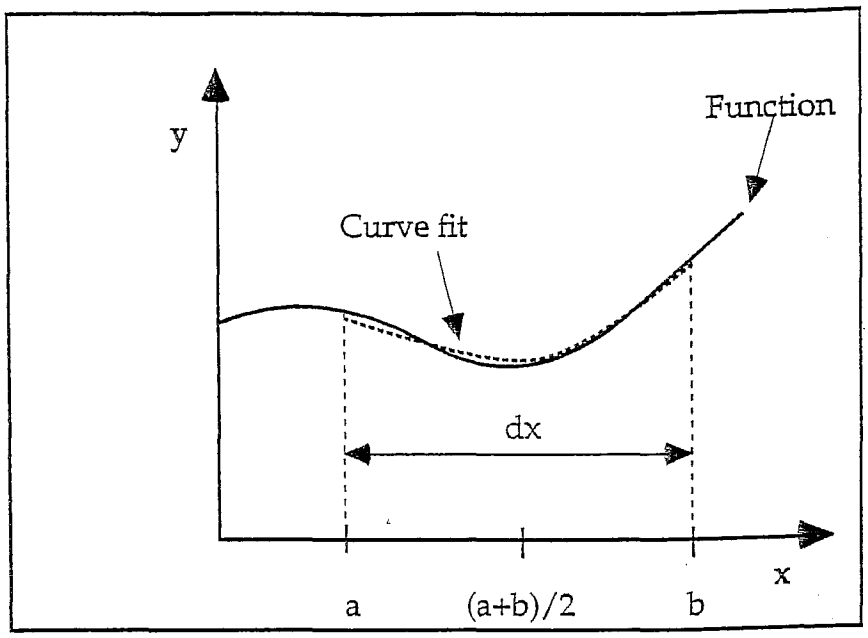

Figure 2.2. Simpson's Rule Curve Fit for One Interval.

The area under the fit for the interval can be shown to be [2]

$$\int_a^b f(x)dx = \frac{b-a}{6}\left[f(a)+4f\left(\frac{a+b}{2}\right)+f(b)\right]$$

where

$$dx = b-a$$

The complete function can be integrated by summing all of the incremental areas for each intervals. It therefore follows that the more intervals (i.e. the smaller dx) the more accurate the integral approximation.

PROPX uses the Simpson's Rule approximation to determine the torque, blade force, and power at each wind speed. These are determined from the following equations

$$Q = \int_{hub}^{tip} \frac{1}{2}\rho W^2 B c C_n r dr$$

$$T = \int_{hub}^{tip} \frac{1}{2}\rho W^2 B c C_t dr$$

$$P = \int_{hub}^{tip} \Omega dQ$$

The integration loop ends by summing the intervals calculated by these equations.

2.7 Thrust and Power Coefficients

With the completion of the integration loop, the major part of the program calculations are finished. The final calculations of the program involve determining the thrust and power coefficients, calculating gap effects (if any), including component efficiencies, converting units and printing output.

The thrust and power coefficients are calculated by the following equations

$$C_T = \frac{T}{\frac{1}{2}\rho V^2 \pi R^2}$$

$$C_P = \frac{P}{\frac{1}{2}\rho V^3 \pi R^2} \qquad (2.1)$$

A modification to the ideal deal power coefficient (equation 2.1) for spaces along the rotor blade is expressed with gap corrections. On blades with partial-span pitch control, trailing vortices result and cause changes in both lift and drag forces. In PROPX this change in power coefficient is given by [3]

$$C_{P_{Available}} = C_{P_{Ideal}} - \Delta C_{P_{Gap}}$$

where

$$\Delta C_{P_{Gap}} = \frac{K x_L \cos^3\psi B c C_L \sin\phi\sqrt{c}}{\pi R}\left[(1-a)^2 + x_L^2(1+a')^2\right]$$

$$K = \frac{2}{R}\sqrt{\frac{s_{Gap}}{12}}$$

S_{Gap} = Location of gap from center of turbine (ft)

2.8 Efficiencies

Because the power calculated by PROPX up to this point is ideal, the efficiencies of the generator and gear box must be included to calculate the electrical output. This is given by

$$P_{Electric} = \frac{-b + \sqrt{b^2 + 4c}}{2}$$

where

$$b = \frac{1}{\left(\frac{1}{\eta_{Gen}} - 1\right)(1-f)}$$

$$c = b\eta_{GB}P_{Rotor} - \frac{P_{Rated}^2 f}{1-f}$$

η_{Gen} = Generator efficiency at rated power (from input file)

η_{GB} = Gear box efficiency (from input file)

P_{Rated} = Rated power (form input file)

f = Fixed loss fraction (from input file)

P_{Rotor} = Rotor power calculated by PROPX

Also calculated in the final stages of the program is the frequency and static displacement of the blade tip at each wind speed. These quantities are calculated in subroutine Check and are not used in the core program. They are simply used to check the blade stiffness and mass data under operating conditions. More on this subroutine is given in section six.

3.0 Subroutine Readfl

The purpose of subroutine Readfl is to read the data from input file that describes the wind turbine. The input file has a simple format to enable users to quickly enter data without having to re-compile and link the program for each new run. It is a standard ASCII text format that is readable by most text editors and word processor programs.

The format of the input file can be divided into two sections. The individual variable data section consists of 31 lines, each with a variable and its constant value (separated by an equals sign). The tabular data section has no set number of lines and contains the blade and elastic data to be interpolated during the integration process.

The subroutine begins by opening the input file (see Figure 3.3). It then reads the 31 lines of individual variable data by calling subroutine Readln. Next the bulk aerodynamic and blade data are read. The order of aerodynamic data is then reversed because the integration scheme begins at the tip and works to the hub. Finally, the radial percentages are turned into decimals to be consistent with the interpolation scheme used later in PROPX.

The purpose of subroutine Readln (shown in Figure 3.4) is to read the individual variable data. It does this by reading a line of text and then converting the numeric portion into a real number. Subroutine Readln "knows" when to start converting the text number to a real number when it finds the equals sign in the line. Everything after the equals sign is converted into a number, so care must be taken not to include any letters of the alphabet, graphic characters, or spaces past this point. See Appendix A: Input File Format for more details.

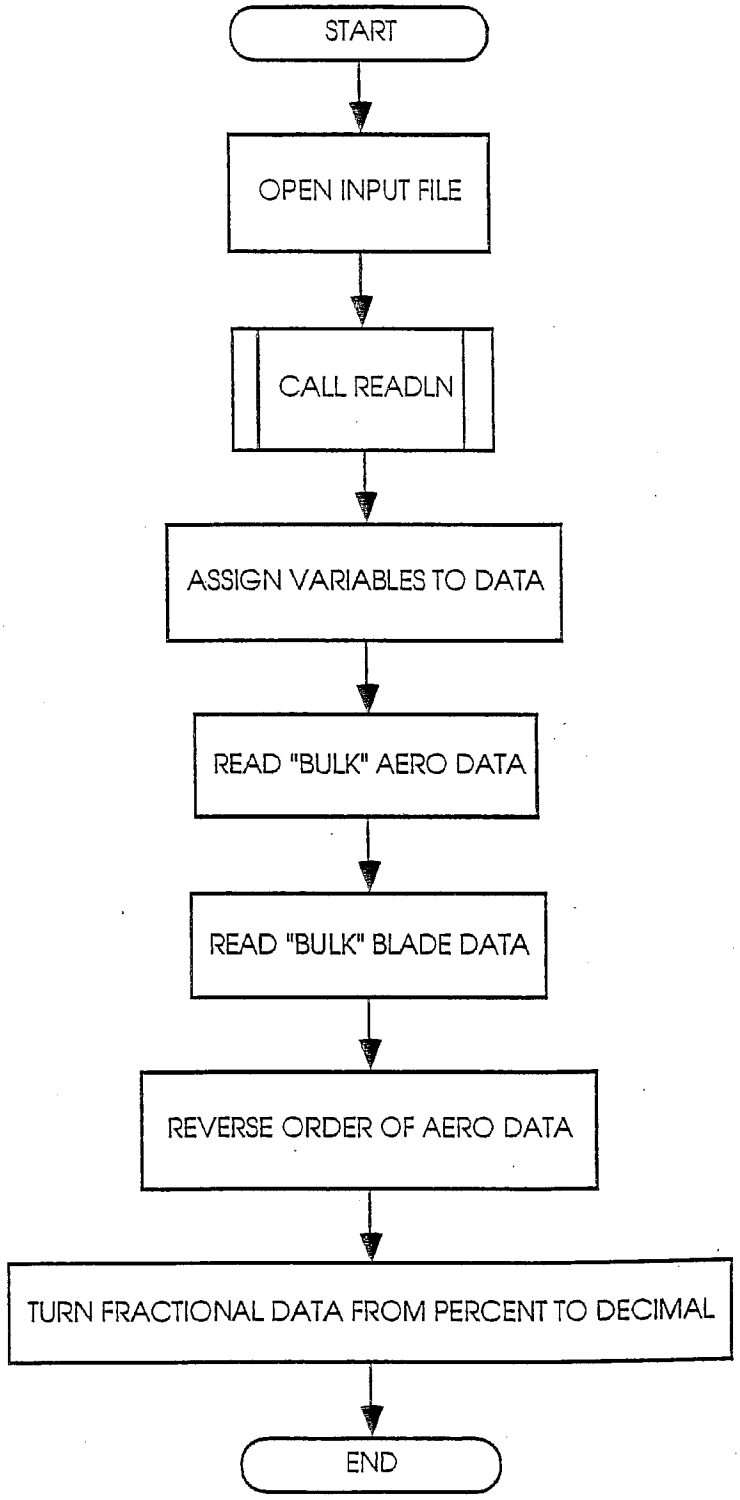

Figure 3.1. Flow Chart for Subroutine Readfl.

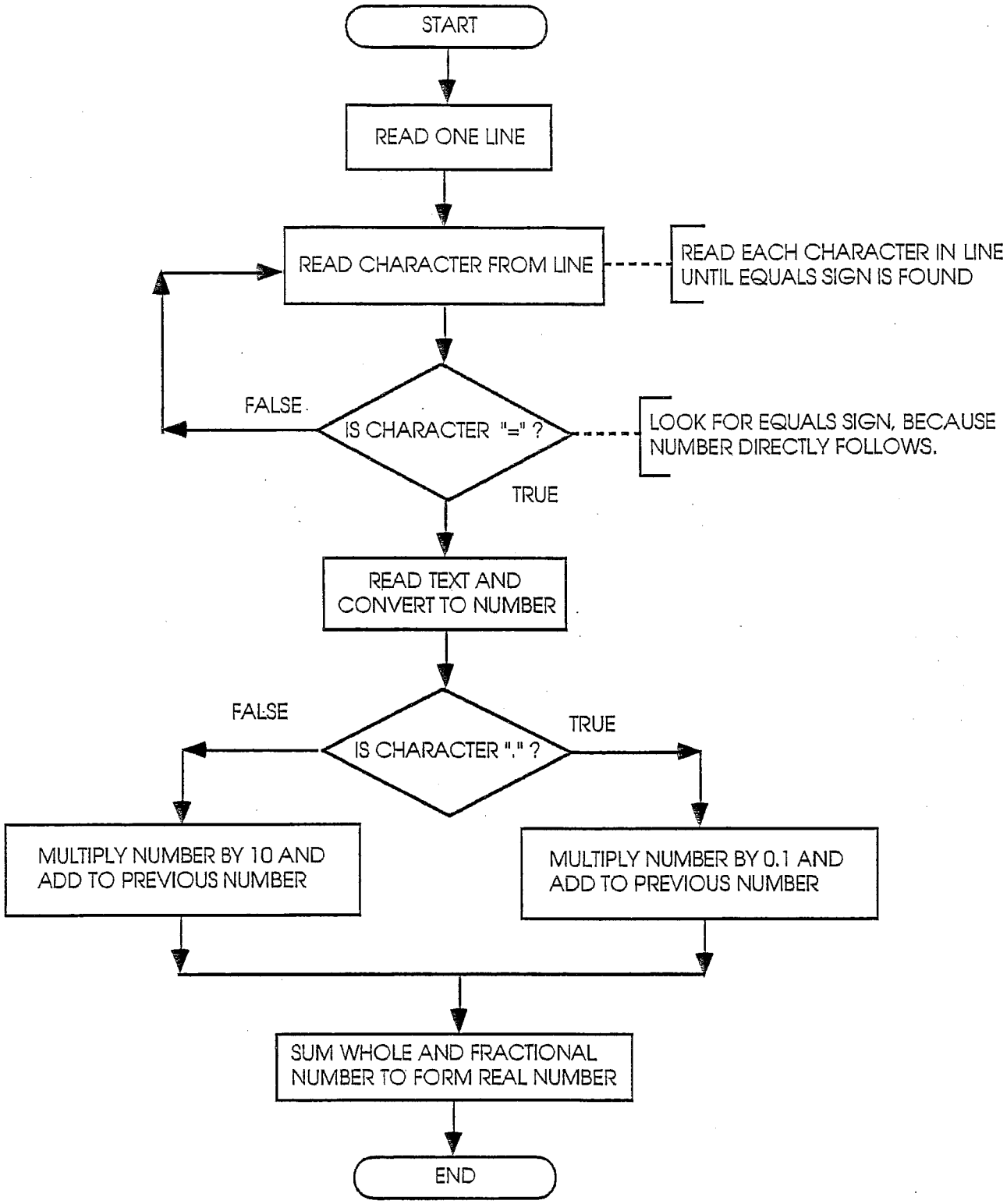

Figure 3.2. Subroutine Readln Called by Subroutine Readfl.

4.0 Subroutine Calc

Subroutine Calc is essentially the heart of PROPX. In it are calculated the quantities necessary to determine the torque and thrust acting on a blade element. Some of the quantities calculated in this subroutine include: relative inflow angle, angle of attack, cascade effects, lift and drag coefficients, tip losses, and induction factors. The derivations for many of these quantities are given in the text to follow. Where derivations become to too lengthy, only a reference is given.

Before a detailed description is given for the above quantities, it is important to first understand the complex logic flow used in Calc. Figure 4.1 shows the flow chart for the subroutine, but the iteration process can be reduced even further to the following six steps:

1. Calculate the relative inflow angle.
2. Calculate angle of attack including cascade effects.
3. Calculate lift and drag coefficients.
4. Calculate new axial induction from blade element/momentum theory equation.
5. Calculate tangential induction.
6. If tolerance between old and new axial induction is not met, iterate again.

From the above short algorithm, it becomes evident that the core of the subroutine involves iterating on the axial induction factor, a, to determine all other quantities. Once the tolerance is met, the relative velocity, thrust, and torque are calculated for the blade section in question. The program then exits the subroutine and increments along the blade to the next radial location, and the whole process starts over again.

4.1 Relative Inflow Angle

Geometrically speaking, the relative inflow angle, ϕ, is the sum of the angle of attack and the twist angle of a rotor blade section. It forms the rotor blade coordinate system known as the n-t system and is shown in Figure 4.2. Other common coordinate systems associated with airfoils are the wind and body axes. In the wind system (also known as the D-L system), the forces on the airfoil are normal and parallel to the local relative velocity, W. In the body system (also known as the N-T system) the forces are normal and parallel to the zero lift line (ZLL) of the airfoil. These too are illustrated in Figure 4.2.

The first step in the iteration process to find the axial induction factor is to find the relative inflow angle. By the geometry of velocity diagram in Figure 4.2, this is given as

$$\tan\phi = \frac{V(1-a)}{r\Omega(1+a')} \tag{4.1}$$

The tangential induction factor, a', is also shown in Figure 4.2. This is sometimes neglected because of its small effect on power. A more detailed analysis of the effects of the tangential induction factor are given at the end of this section.

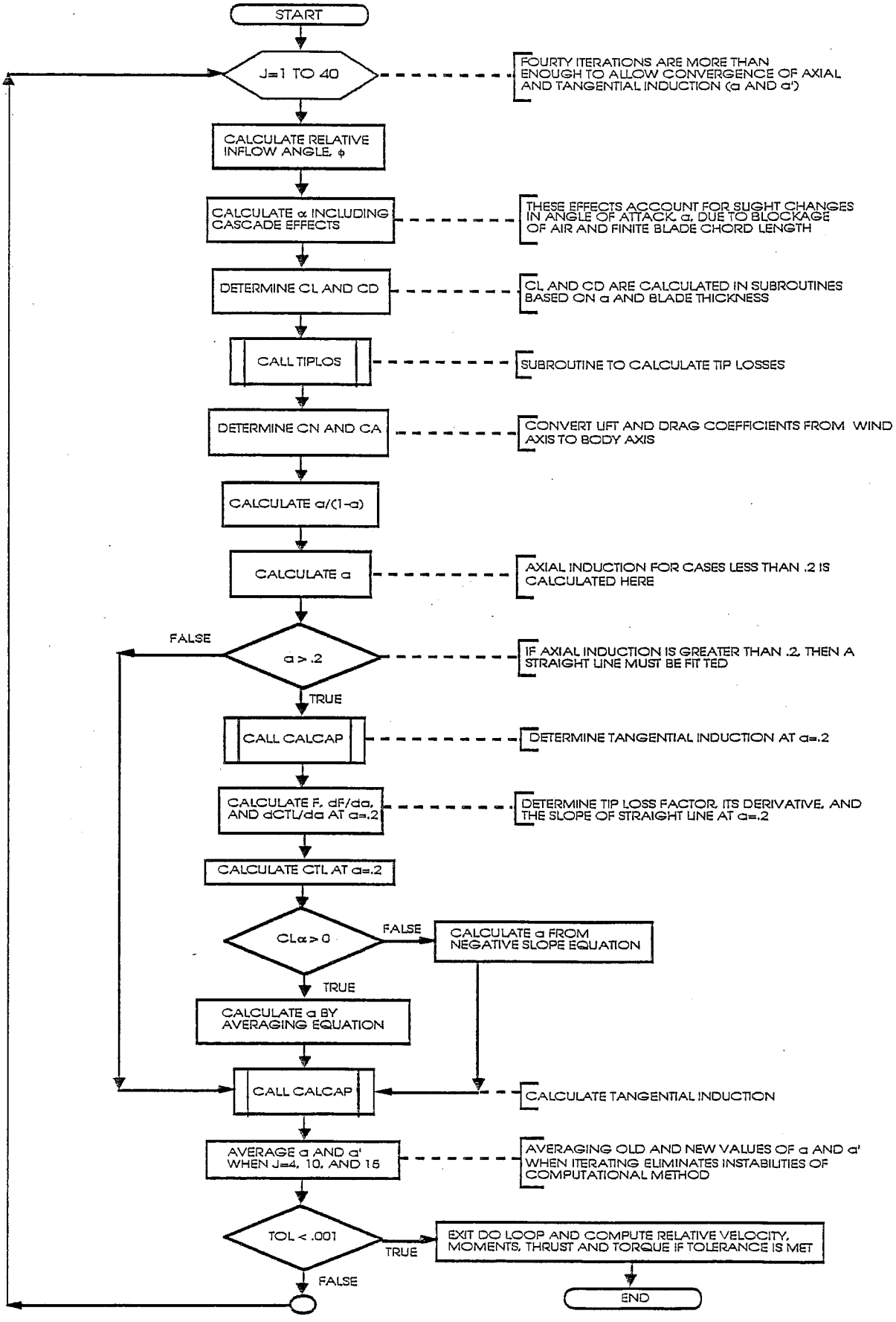

Figure 4.1. Subroutine Calc Flow Chart.

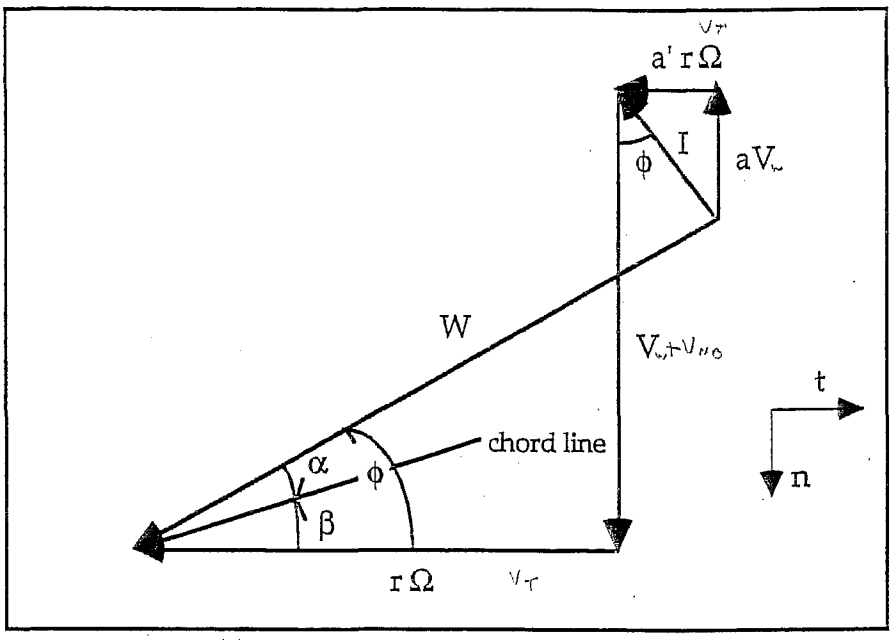

Figure 4.2. Velocity Diagram of Wind Turbine Blade Section.

4.2 Angle of Attack

The angle of attack is used to determine the lift and drag coefficients, which in turn are used to determine the forces acting on the blade. As mentioned earlier, the angle of attack is the angle between the local relative velocity and the chord line of the airfoil. Because the velocity and twist vary along the turbine blade, this angle too varies.

It is desirable, but impossible to keep the angle of attack along the blade out of the stall region, which is an area reduced lift and increased drag at high angles of attack. Although there is always be a region of stall on some portion of blade surface, stall effects can be reduced by twisting the blade to an appropriate angle that minimizes flow separation. Higher twist near the hub and low twist at the tip is the norm.

Once PROPX determines the relative inflow angle, the angle of attack is determined from

$$\alpha = \phi - \beta$$

The twist angle, β, comes from the input file. During the iteration process, twist is determined by interpolation based on the radial location of the blade segment.

4.3 Cascade Effects

The effects of the finite width of the rotor and the thickness of the blade give rise to changes in angle of attack known as cascade effects. As the turbine blade passes through the wake of the previous blade, these effects cause streamline curvature and streamline displacement. The higher the solidity, (essentially the greater the chord length and number of blades) the more these corrections are needed.

The curvature of the flow due to the finite cord width of the rotor causes a change in the circulation developed by the blades [3]. This change in circulation causes a decrease in angle of attack given by

$$\Delta\alpha_1 = \frac{1}{4}\left[\tan^{-1}\frac{(1-a)V}{(1+2a')r\Omega} - \tan^{-1}\frac{(1-a)V}{r\Omega}\right]$$

The second of the cascade effects results from the thickness of the airfoil. A thick airfoil will cause blockage of the flow, which by continuity, will cause the flow to accelerate and effectively increase the angle of attack of the next blade to flow through the accelerated wake. This change causes an increase in angle of attack and is given by

$$\Delta\alpha_2 = .109\frac{Bct_{MAX}X}{Rc_l\sqrt{(1-a)^2+\left(\frac{rX}{R}\right)^2}}$$

where

R = Total blade radius

$$X = \frac{R\Omega}{V}$$

c = Chord length

PROPX applies these corrections to the angle of attack computed from the twist and relative inflow discussed earlier. The new angle of attack is computed in the following manner

$$\alpha_{Cascade} = \alpha + \Delta\alpha_1 + \Delta\alpha_2$$

4.4 Aerodynamic Coefficients

Once the angle of attack is calculated with cascade effects, the lift and drag coefficients can be determined. In PROPX this is done by a call to an airfoil subroutine (see next section on airfoil subroutines). The airfoil subroutine computes a C_L and C_D based on the local angle of attack and thickness. Because C_L and C_D are expressed in the wind coordinate system, they must transformed into the n-t system, which is necessary for the determination the induction factors. These transformations are given by

$$C_n = C_L\cos\phi + C_D\sin\phi$$

$$C_t = C_L\sin\phi - C_D\cos\phi$$

4.5 Tip Loss Factor

The Prandtl tip loss factor, F, is used to model the loss in aerodynamic force due to the interaction of shed vorticity with bound vorticity. Because the torque produced at the tips of the rotor blade is a major contributor to power, such a correction is essential. This is given by [3]

$$F = \frac{2}{\pi}\cos^{-1}(e^{-f})$$

where

$$f = \frac{B}{2}\frac{R-r}{R\sin\phi}$$

4.6 Axial and Tangential Induction Factors

The axial and tangential induction factors are dimensionless quantities which express the decrease in axial and increase in tangential velocities at the rotor blade. Both of these changes result from the induced velocity vector (denoted by I in Figure 4.2) caused by the trailing tip vortex.

Just before entering the rotor blade, the velocity, U, can be expressed as the average of the free stream velocity, V, and the far wake velocity, V_2, (see Figure 4.3). This average represents a decrease in velocity due to the expenditure of kinetic energy in turning the rotor blade. The decrease in free stream velocity at the rotor forms the normal component of relative velocity and can therefore be expressed in terms of the axial induction factor [3]

$$W_n = U = V(1-a)$$

The increase in the tangential component of velocity can be expressed in terms of the tangential induction factor

$$W_t = r\Omega(1+a')$$

Also, the velocity of the far wake can be expressed as

$$V_2 = V(1-2a)$$

Note that W_t is not illustrated in Figure 4.3 because it is normal to, and pointing out of the plane of the paper for the rotor turning from top to bottom.

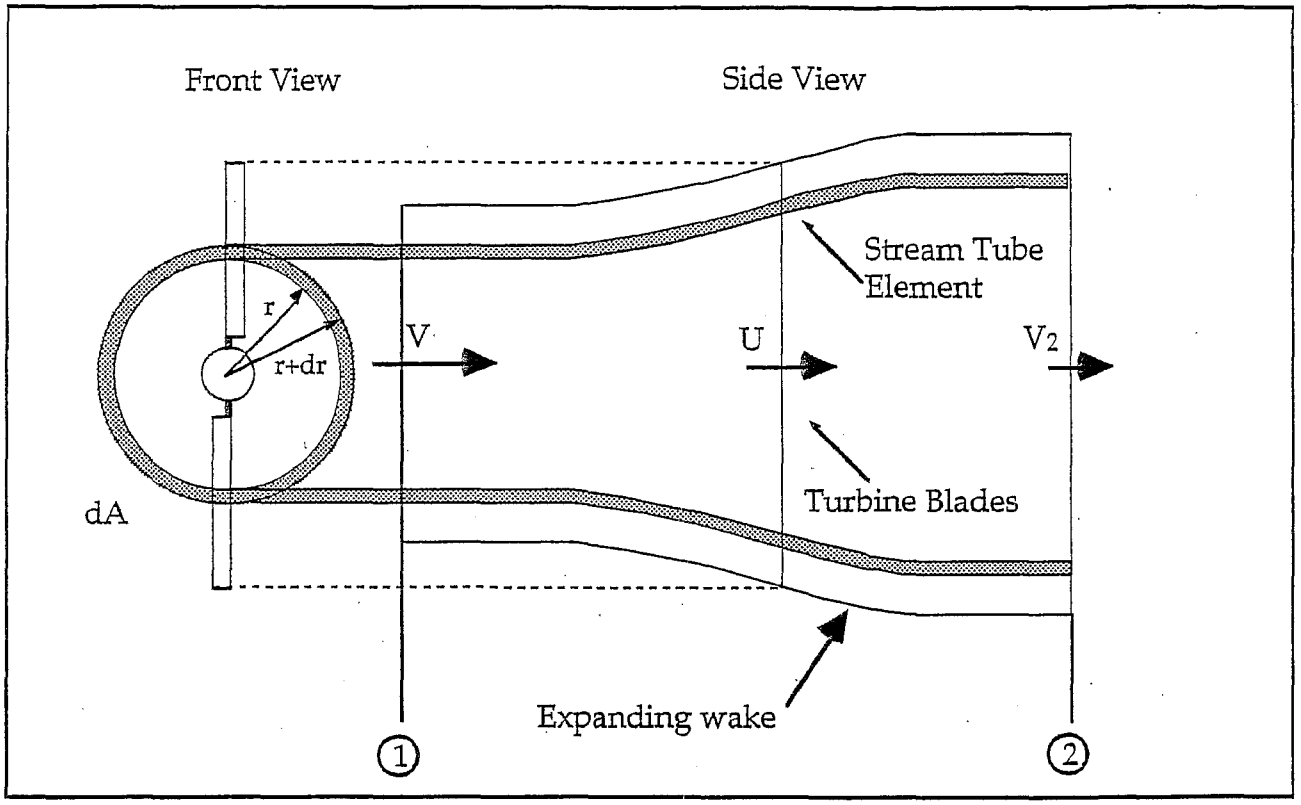

Figure 4.3. Control Volume for Wind Turbine Wake.

The axial induction factor, a, can be determined by equating the momentum flux through the annular area in Figure 4.3 to the blade force caused by circulation of the wind around the blade [3]. The momentum flux equation will be considered first. For the control volume between stations 1 and 2 the flux is given by

$$dT_{momentum} = d\dot{m}\Delta V_{axial} = \rho U \Delta V_{axial} dA \qquad (4.2)$$

Where

$$\Delta V_{axial} = 2aV \qquad (4.3)$$

$$dA = 2\pi r dr \cos^2\psi \qquad (4.4)$$

The effect of coning angle, ψ, in the above equation is shown in Figure 4.4. Coning is a design modification to allow the rotor blades to be tilted away from the wind to relieve excessive wear on the rotor shaft. This causes a small decrease in power generation, with the benefit of extended turbine lifetime. Because PROPX includes this effect in calculations, the term, $\cos\psi$, will seen in equations throughout this text.

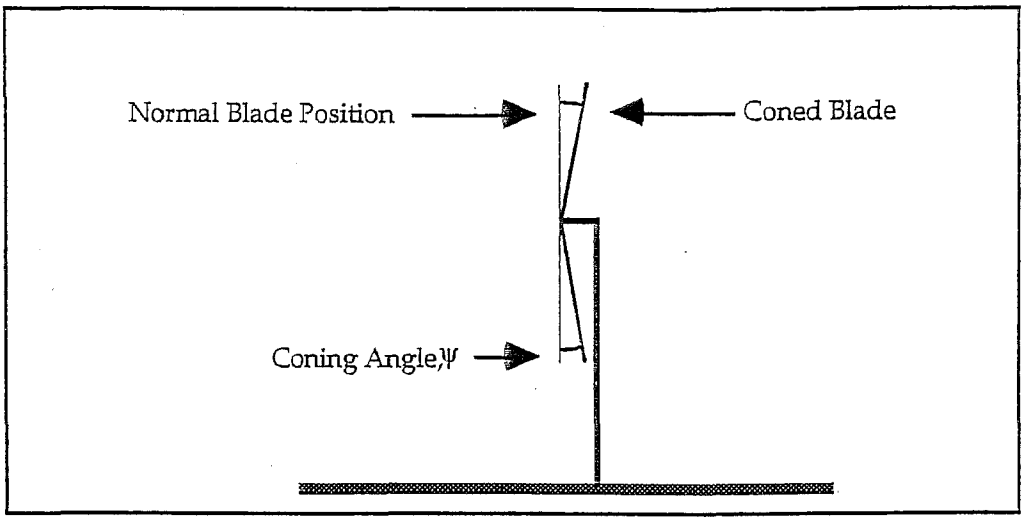

Figure 4.4 Illustration of a Coned Turbine Blade.

Once equations (4.3) and (4.4) are substituted into equation (4.2), the momentum flux through the coned blade becomes

$$dT = 4\pi r\rho V^2 a(1-a)\cos^2\psi dr \qquad (4.5)$$

With an expression for the momentum flux now available, an expression for the normal component of the blade force, F_n, has to be found. This force is illustrated in Figure 4.5.

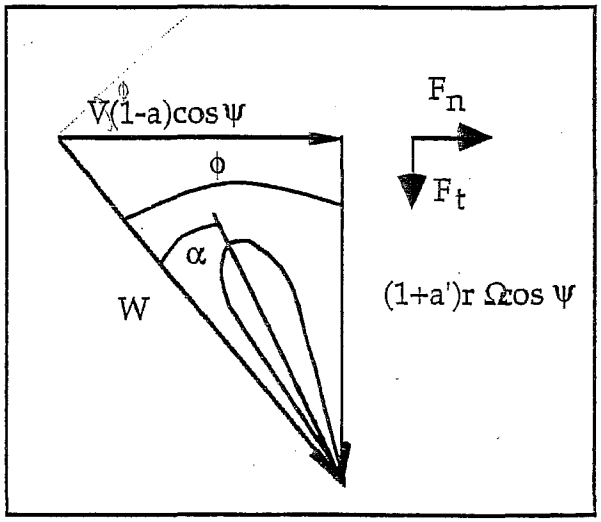

Figure 4.5. Normal and Tangential Forces Acting on Blade Surface.

The normal force component acting on a coned blade can be determined from circulation considerations [3], which are given by

$$dF_n = dT_{Blade} = \frac{1}{2}B\rho W^2 c C_L \cos\phi\cos\psi dr$$

By Figure 4.5

$$\sin\phi = \frac{V(1-a)\cos\psi}{W} \quad \text{or} \quad W = \frac{V(1-a)\cos\psi}{\sin\phi} \tag{4.6}$$

Inserting equation (4.7) into the blade force equation gives

$$dT = \frac{1}{2}B\rho\left(\frac{V(1-a)\cos\psi}{\sin\phi}\right)^2 cC_L \cos\phi\cos\psi dr \tag{4.7}$$

Now that equations for both the blade force and momentum flux equations are known, they can be equated to each other to find the axial induction factor. Equating equations (4.5) and (4.7) gives

$$4\pi r\rho V^2 a(1-a)\cos^2\psi dr = \frac{1}{2}B\rho\left(\frac{V(1-a)\cos\psi}{\sin\phi}\right)^2 cC_L \cos\phi\cos\psi dr \tag{4.8}$$

Canceling like terms gives

$$4\pi ra = \frac{1}{2}B\frac{\cos\phi}{\sin^2\phi}(1-a)cC_L \cos\psi$$

Rearranging gives

$$\frac{a}{1-a} = \frac{BcC_L \cos\phi\cos\psi}{8\pi r\sin^2\phi}$$

If the axial induction is solved for, then

$$a = \frac{K}{1+K} \tag{4.9}$$

where

$$K = \frac{BcC_L \cos\phi\cos\psi}{8\pi r\sin^2\phi} \tag{4.10}$$

Equations similar to (4.9) and (4.10) are used in PROPX to find the axial induction during the iteration process. Since all the terms in K are available through airfoil lookups, input data, or previous calculations, the solution of axial induction becomes one of mass multiplication.

Alternately, the local thrust coefficient can be found [4] beginning with equation (4.8) and inserting

$$C_{T_L} = 4a(1-a)$$

which gives

$$2\pi r\rho V^2 C_{T_L}\cos^2\psi dr = B\rho W^2 c C_L \cos\phi\cos\psi dr$$

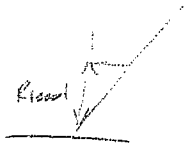

After solving for the local thrust coefficient

$$C_{T_L} = \frac{BW^2 c C_L \cos\phi}{2\pi r V^2 \cos\psi} \tag{4.11}$$

From Figure 4.5

$$\cos\phi = \frac{(1+a')r\Omega\cos\psi}{W} \tag{4.12}$$

and

$$W = \sqrt{[V(1-a)\cos\psi]^2 + [(1+a')r\Omega\cos\psi]^2} \tag{4.13}$$

Inserting (4.13) and (4.12) into (4.11) gives

$$C_{T_L} = \frac{BcC_L\Omega(1+a')\cos\psi}{2\pi V}\sqrt{(1-a)^2 + (1+a')^2 x^2}$$

And finally, the form used by PROPX

$$C_{T_L} = \frac{BcC_L X(1+a')\cos\psi}{2\pi R}\sqrt{(1-a)^2 + (1+a')^2 x^2} \tag{4.14}$$

A similar form of equation (4.10) can be found for the tangential induction, a', by equating the moment of momentum with the blade torque. Beginning with the moment of momentum

$$dQ_{\text{Angular Momentum}} = d\dot{m}V_t r = \rho U r V_t dA\cos\psi \tag{4.16}$$

where

$$d\dot{m} = \rho U dA$$

$$U = V(1 - a)$$

$$V_t = r\omega\cos\psi$$

$$dA = 2\pi r dr \cos^2\psi$$

Once the above three equations are substituted into equation (4.16), the momentum of momentum through the coned blade becomes

$$dQ_{Momentum} = 4\pi r^3 \rho V(1-a)a'\Omega dr\cos^4\psi$$

where

$$a' \equiv \frac{\omega}{2\Omega}$$

The blade torque, analogous to the blade force in momentum derivation, can equated to the moment of momentum determined above. The blade torque equation uses the tangential force component, F_t, multiplied by a moment arm.

$$dF_t r = dQ_{Blade} = \frac{1}{2} r\cos\psi\rho W^2 BcC_L \sin\phi dr$$

after inserting equation (4.6) this reduces to

$$Q = \frac{1}{2} r\cos^3\psi\rho V^2(1-a)^2 BcC_L \frac{1}{\sin\phi} dr$$

When the moment of momentum is equated to the blade torque

$$Q_{Momentum} = Q_{Blade}$$

$$4\pi\rho V(1-a)r^3\cos^4\psi a'\Omega dr = \frac{1}{2} rB\rho cV^2(1-a)^2 C_L \frac{\cos^3\psi}{\sin\phi} dr$$

canceling, rearranging, and solving for a' gives

$$a' = \frac{BcV(1-a)C_L}{8\pi r^2\cos\psi\Omega\sin\phi}$$

recall that

$$\tan\phi = \frac{V(1-a)}{(1+a')r\Omega} \quad \text{or} \quad V(1-a) = (1+a')r\Omega\tan\phi \tag{4.16}$$

so

$$a' = \frac{Bc\tan\phi(1+a')C_L}{8\pi r\cos\psi\cos\phi}$$

therefore

$$\frac{a'}{1+a'} = \frac{BcC_L}{8\pi r\cos\psi\cos\phi} \tag{4.17}$$

The tangential induction in (4.18) can be solved for similar to the case of axial induction in equations (4.10) and (4.11), but for reasons to be explained later this equation is not used in PROPX. The desired form is to have tangential induction expressed as a function of axial induction. This can be constructed by first considering the induced velocity, I, in Figure 4.2 caused by the rotor tip vortex. By this geometry, the relative inflow angle for a coned blade can be expressed as

$$\tan\phi = \frac{a'r\Omega\cos\psi}{aV} = \frac{V(1-a)}{r\cos\psi\Omega(1+a')}$$

Canceling and rearranging terms gives

$$a'x^2\cos^2\psi(1+a') = a(1-a)$$

By multiplying out terms and rearranging further, a form suitable for the Quadratic Formula can be constructed

$$x_L^2(a')^2 + x_L^2a' - a(1-a) = 0$$

where

$$x_L = \frac{r\cos\psi\Omega}{V}$$

applying the Quadratic Formula the above results in

$$a' = \frac{-x_L \pm \sqrt{x_L^2 + 4a(1-a)}}{2x_L}$$

This can be further reduced to the form used by PROPX

$$a' = \frac{1}{2}\left[\sqrt{1+\frac{4a(1-a)}{x_L^2}} - 1\right] \tag{4.18}$$

Equation (4.18) is identical to the equation used in subroutine Calcap called by subroutine Calc. Equation (4.17) is not used to calculate a' because first derivative of (4.18) with respect to axial induction is required in a later derivation. The derivative of equation (4.18) can be readily determined by simple calculus to be

$$\frac{\partial a'}{\partial a} = \frac{1-2a}{x_L^2(1+2a')} \tag{4.19}$$

4.7 Momentum Equation Correction

When the axial induction factor is greater than 0.2, the momentum equation begins to lose its integrity when compared with empirical results because of wake expansion effects. To correct for this, a straight line is fit to the momentum solution at values of a > 0.2. This is shown in Figure 4.6.

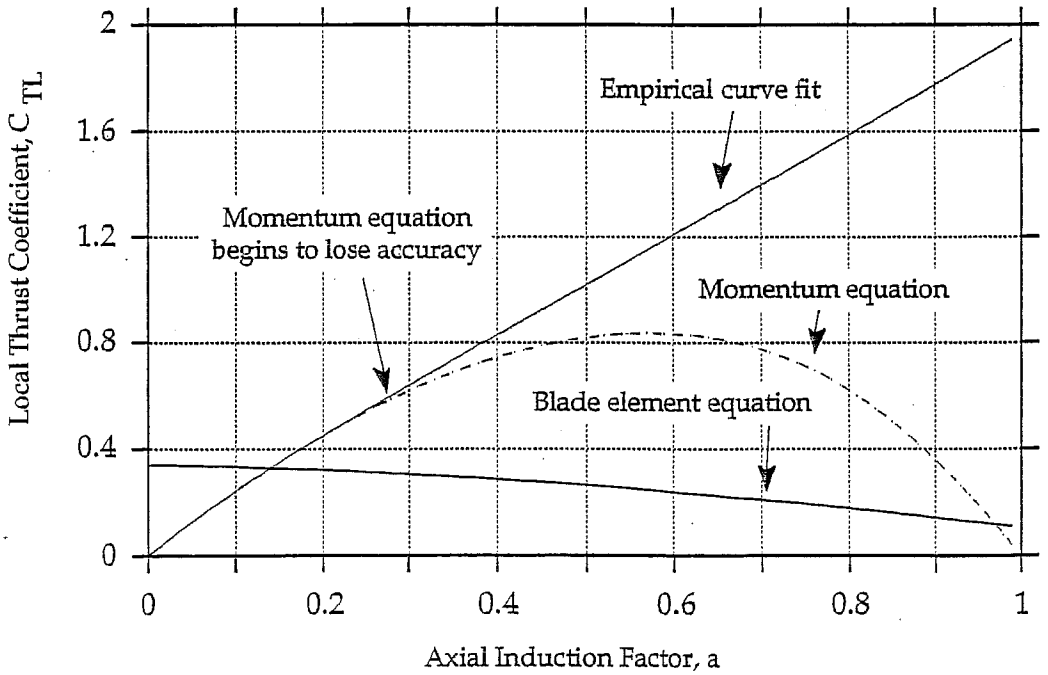

Figure 4.6. Comparison of Empirical, Momentum, and Blade Element Equations.

The local thrust coefficient for all values of axial induction can thusly be described by

$$C_{T_L} = 4aF(1-a) \qquad \text{for } a \le a_c \qquad (4.20)$$

$$C_{T_L} = C_{T_L}\Big|_{a=0.2} + \left.\frac{\partial C_{T_L}}{\partial a}\right|_{a=0.2} (a - 0.2) \qquad \text{for } a > a_c$$

$$\begin{array}{ccc} \Uparrow & \Uparrow & \Uparrow \\ 1 & 2 & 3 \end{array} \qquad (4.21)$$

Subroutine Calc uses equation (4.21) to determine axial induction at values greater than a_c. Because Calc iterates on axial induction, this equation is rearranged and solved for as

$$a = a_c - \frac{C_{T_L}\Big|_{ac} - C_{T_L}}{\left.\frac{\partial C_{T_L}}{\partial a}\right|_{ac}} \qquad (4.22)$$

where

$$a_c = 0.2$$

Each of the terms in equation (4.21) can be determined individually. Term 1 is the solution to the blade element equation in terms of the local thrust coefficient. This has already been determined in equation (4.15) to be

$$C_{T_L} = \frac{BcC_L X(1+a')\cos\psi}{2\pi R}\sqrt{(1-a)^2 + (1+a')^2 x^2} \qquad (4.23)$$

Term 2 is the local thrust coefficient at a_c, which is simply the momentum solution at $a = a_c$.

$$C_{T_L}\Big|_{ac} = 4a_c F_c(1-a_c) \qquad (4.24)$$

Term 3 is the derivative of the local thrust coefficient with respect to axial induction. Taking this derivative involves taking the derivatives of other functions also dependent upon the axial induction factor. These functions include the tip loss factor, tangential induction factor, and relative inflow angle. These derivatives are given below.

Beginning with the momentum solution, and taking its derivative by implicit differentiation

$$\left.\frac{\partial C_{T_L}}{\partial a}\right|_{ac} = \frac{\partial}{\partial a}\left[4a_c F_c(1-a_c)\right] = 4F_c(1-2a_c) + 4a_c\frac{\partial F_c}{\partial a}(1-a_c) \tag{4.25}$$

To find the derivative of the tip loss factor, F, its equation can be rearranged to be

$$\cos\left(\frac{\pi F}{2}\right) = \exp\left[-\frac{B(R_L - r_L)}{2R_L \sin\phi}\right] \tag{4.26}$$

After implicit differentiation, this becomes

$$-\frac{\pi}{2}\frac{\partial F}{\partial a}\sin\left(\frac{\pi F}{2}\right) = \exp\left[-\frac{B(R_L - r_L)}{2R_L \sin\phi}\right]\left[-\frac{B(R_L - r_L)}{2R_L \sin\phi}\right]\left[-\frac{\cos\phi}{\sin\phi}\right]\frac{\partial\phi}{\partial a}$$

Solving for the derivative and re-inserting equation (4.26) gives

$$\frac{\partial F}{\partial a} = -\frac{B}{\pi}\cot\left(\frac{\pi F}{2}\right)\left(\frac{R_L - r_L}{R_L}\right)\left(\frac{\cos\phi}{\sin\phi}\right)\frac{\partial\phi}{\partial a} \tag{4.27}$$

Because the relative inflow angle in equation (4.27) is a function of axial induction, its derivative must too be found. Starting with equation (4.1)

$$\tan\phi = \frac{V(1-a)}{(1+a')r\Omega} \tag{4.1}$$

After implicit differentiation, this becomes

$$\sec^2\phi\frac{\partial\phi}{\partial a} = -\frac{\cos\psi}{(1+a')x_L} - \frac{(1-a)\cos\psi}{(1+a')^2 x_L}\frac{\partial a'}{\partial a}$$

Re-inserting equation (4.1) and rearranging gives

$$\frac{\partial\phi}{\partial a} = -\cos^2\phi\tan\phi\left(\frac{1}{1-a} + \frac{1}{1+a'}\frac{\partial a'}{\partial a}\right) \tag{4.28}$$

Recalling that the derivative of tangential induction with respect to axial induction in (4.28) was determined with equation (4.19). Combining these two gives

$$\frac{\partial\phi}{\partial a} = -\cos\phi\sin\phi\left(\frac{1}{1-a} + \frac{1}{1+a'}\frac{1-2a}{x_L^2(1+2a')}\right)$$

This reduces to

$$\frac{\partial\phi}{\partial a}=\frac{-\cos\phi\sin\phi}{1-a}\left(1+\frac{1-2a}{1+2a'}\frac{a'}{a\cos^2\psi}\right) \tag{4.29}$$

Inserting (4.29) into (4.27) gives

$$\frac{\partial F}{\partial a}=-\frac{B}{\pi}\cot\left(\frac{\pi F}{2}\right)\left(\frac{R_L-r_L}{R_L}\right)\left(\frac{\cos\phi}{\sin\phi}\right)\left(\frac{-\cos\phi\sin\phi}{1-a}\right)\left(1+\frac{1-2a}{1+2a'}\frac{a'}{a\cos^2\psi}\right)$$

Which reduces to

$$\frac{\partial F}{\partial a}=\frac{B}{\pi}\frac{1}{\tan\left(\frac{\pi F}{2}\right)}\left(\frac{R_L-r_L}{R_L}\right)\left(\frac{\cos^2\phi}{\sin\phi}\right)\left(1+\frac{a'(1-2a)}{(1+2a')a\cos^2\psi}\right) \tag{4.30}$$

When (4.30) is inserted into (4.25), the slope of the curve fit as a function of the axial induction factor results.

$$\left.\frac{\partial C_{T_L}}{\partial a}\right|_{ac}=4F_c(1-2a_c)+4a_c\frac{B}{\pi}\frac{1}{\tan\left(\frac{\pi F_c}{2}\right)}\left(\frac{R_L-r_L}{R_L}\right)\left(\frac{\cos^2\phi_c}{\sin\phi_c}\right)\left(1+\frac{a_c'(1-2a_c)}{(1+2a_c')a_c\cos^2\psi}\right)(1-a_c)$$

Where a subscript of "c" indicates a at 0.2 and a subscript of "L" indicates a multiplication by $\cos\psi$, the coning angle.

To understand the complexity of the correction to the momentum equation when an expanding wake is considered, equation (4.22) can be filled in with equations (4.23), (4.24), and (4.30) to become

$$a=a_c-\frac{[4a_cF_c(1-a_c)]-\left[\frac{BcC_LX(1+a')\cos\psi}{2\pi R}\sqrt{(1-a)^2+(1+a')^2x^2}\right]}{4F_c(1-2a_c)+4a_c\frac{B}{\pi}\frac{1}{\tan\left(\frac{\pi F_c}{2}\right)}\left(\frac{R_L-r_L}{R_L}\right)\left(\frac{\cos^2\phi_c}{\sin\phi_c}\right)\left(1+\frac{a_c'(1-2a_c)}{(1+2a_c')a_c\cos^2\psi}\right)(1-a_c)}$$

Although this solution is quite complicated in appearance, it does represent an expression for the axial induction factor that can be evaluated with data available from the input file.

4.8 Computational Instabilities

After the induction factors are calculated they are averaged with values from the previous iteration. This is done to prevent the iteration process from oscillating about the correct answer, but never reaching it. This strictly to prevent computational instabilities and has no physical meaning associated with wind turbine performance.

4.9 Final Calculations

When PROPX finishes iterating on the axial induction factor, the torque and force acting on the blade element can be determined. These are determined from

$$Q = \frac{1}{2} B \rho W^2 c C_t r \cos\psi$$

$$T = \frac{1}{2} B \rho W^2 c C_n \cos\psi$$

where W is calculated from equation (4.13)

Upon exiting subroutine Calc, the torque and force at the blade section are summed to values calculated on the previous section. This process stops when the blade hub is reached.

4.10 The Effect of the Tangential Induction Factor

In some wind turbine performance prediction codes the effect of the tangential induction factor is neglected. This is normally done to reduce computational time with little effect on prediction methods. With today's high speed computers this effect can be included to increase accuracy with a negligible increase in computational time.

Figure 4.7 shows the effect on power with and without the tangential induction factor. It is evident from the plot that there is little difference between the two cases at low wind speeds. At wind speeds greater than approximately 30 MPH, however; the curves begin to diverge, and at 50 MPH there is a difference of about 11 kW. This increase in power at high wind speeds associated with tangential induction results from a decrease in angle of attack, α, and an increase in dynamic pressure shown in Figures 4.8 and 4.9.

The change in angle of attack and dynamic pressure can be traced to increases in both induction factors. The effect these increases have on angle of attack and relative velocity is shown in exaggerated velocity diagrams in Figure 4.10. Since both induction factors are bigger, the normal component of the relative velocity vector decreases and the tangential component increases, causing a reduction in angle of attack. Furthermore, because the decrease in the normal velocity component is not as great as the increase in the tangential velocity component, the relative velocity also increases. Because the dynamic pressure is essentially a constant multiplied the relative velocity squared, it too must increase.

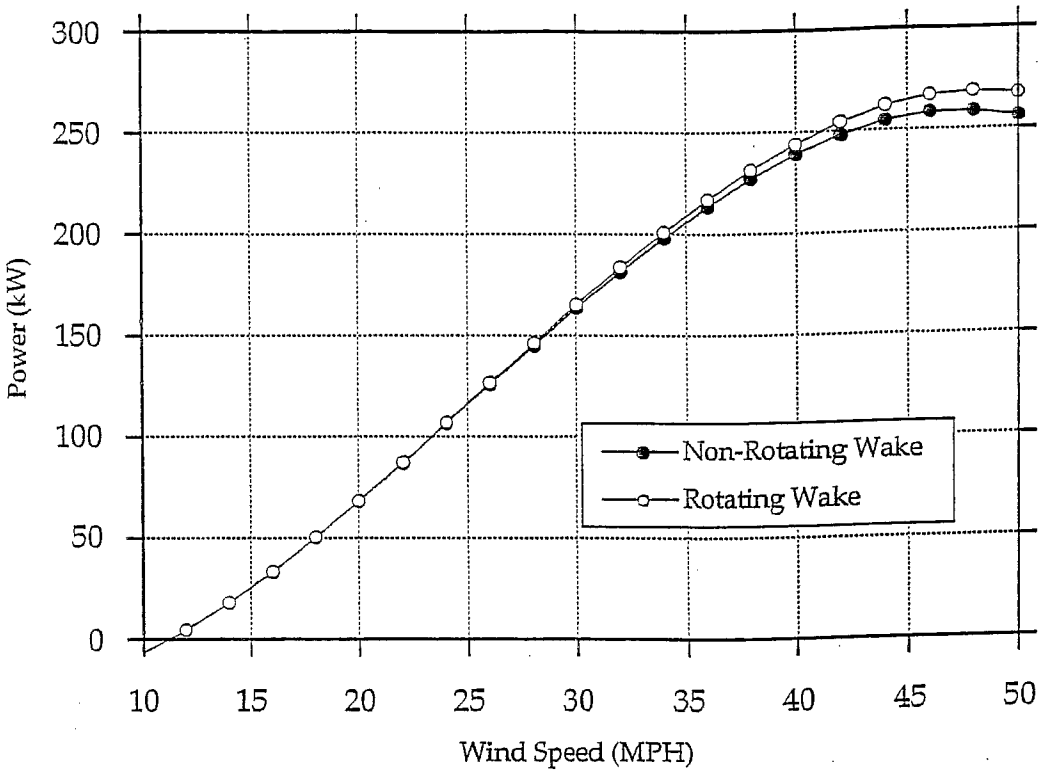

Figure 4.7. Comparison of Power Produced by ESI-80 Turbine when Considering Both Rotating and Non-rotating Wakes.

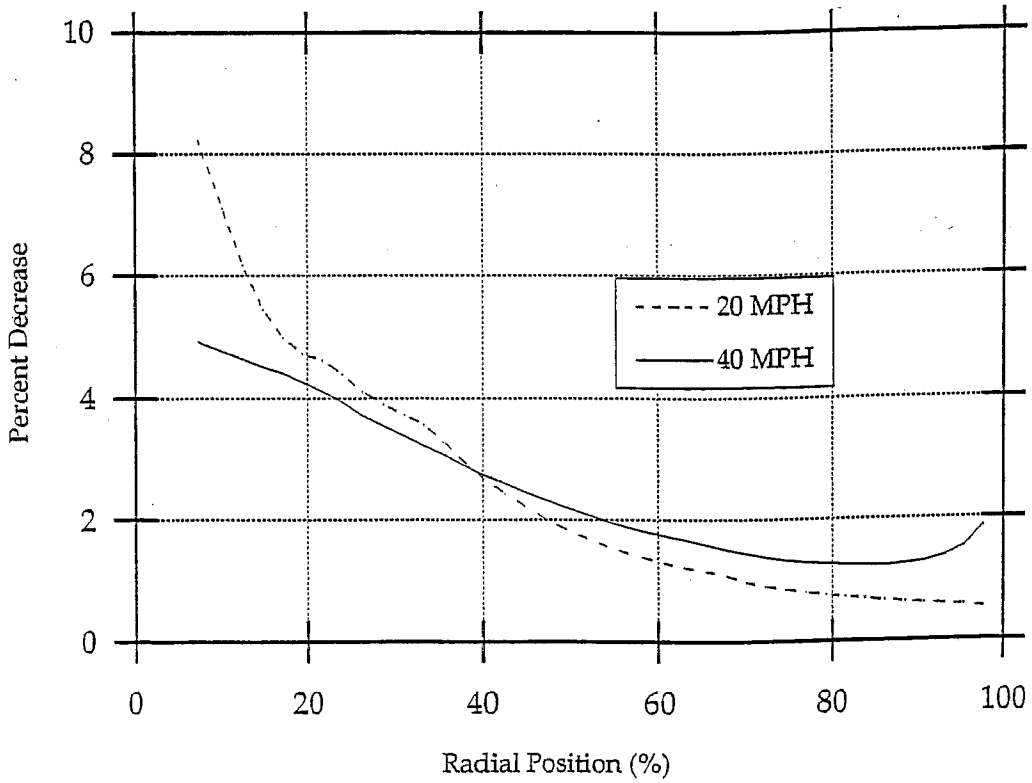

Figure 4.8. Percent Decrease in Angle-of-attack along Blade due to Tangential Induction at 20 and 40 MPH.

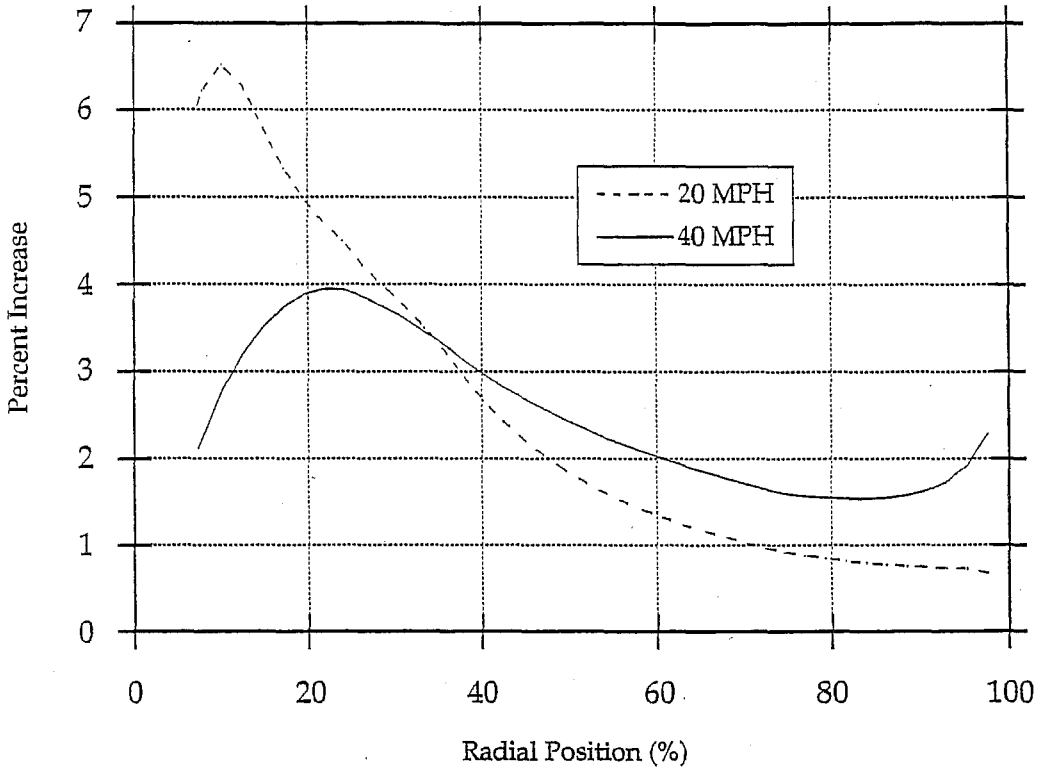

Figure 4.9. Percent Increase in Dynamic Pressure along Blade Due to Tangential Induction at 20 and 40 MPH.

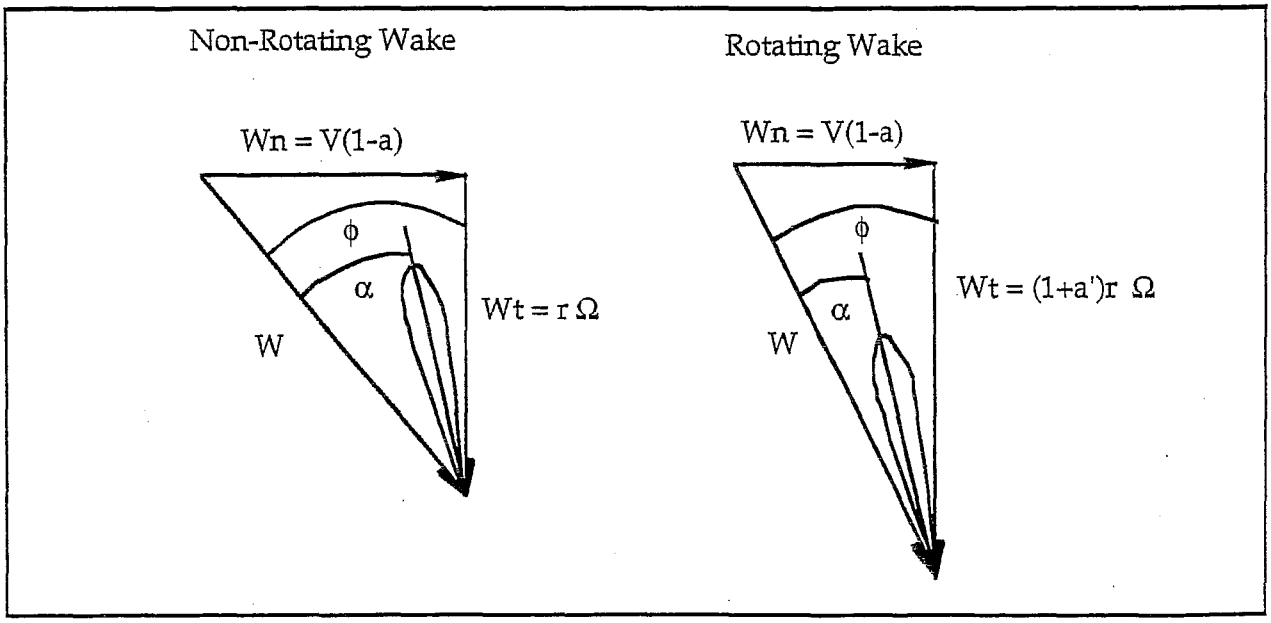

Figure 4.10. Velocity Diagrams of Turbine Blade Sections.

5.0 Airfoil Subroutines

In PROPX there are currently three options to choose from in the area of inputting airfoil data. These include two "built-in" airfoil subroutines and the option of a user created data file for inputting wind tunnel data for other airfoils. The airfoils specially modeled in PROPX include the NACA 23000 and the LS(1) and are shown in Figure 5.1. These are included because they are commonly used on wind turbines.

The two airfoils modeled in the program are based on curve fits and extrapolations from wind tunnel data. These curve fits produce the characteristic C_L-α and C_D-C_L plots which are functions of angle of attack and the maximum airfoil thickness. Rather than going through the derivation and flow charts of these subroutines, only plots of the output are provided. These plots show the effect of varying the thickness on the lift, drag, and tangential coefficients.

Thickness is varied along the turbine blade because sections may have an angle of attack that is past the stall limit. A thick airfoil will have a greater leading edge radius which will guide the flow better and resist the effects of flow separation better than a thin airfoil [3]. A thin airfoil is used in areas that have a low angle of attack (towards the blade tip), because a thin airfoil will have a greater maximum lift coefficient. Once past stall, however; the lift coefficient for a thin airfoil will drop much faster than for a thick airfoil.

5.1 NASA LS(1) Airfoil

The LS(1) is an advanced NASA airfoil designed in the 1970s. Unlike previous airfoils designed by wind tunnel trial-and-error testing, the LS(1) was designed by computational methods. Characteristically, this airfoil has a larger leading edge radius to flatten the sharp peak associated with the pressure coefficient near the nose (see Figure 5.1). It also has a cuisped trailing edge on the bottom surface to increase the loading in that region. These design features decrease the effects of flow separation at high angles of attack and therefore increase the lift coefficient. Data for this airfoil at varying values of t_{max}/c and angle of attack is shown in Figures 3.2-3.4.

5.2 NACA 23000 Airfoil

The NACA 23000 airfoil was developed much earlier than the LS(1) and its development was based on wind tunnel test data rather than computer modeling. The 23000 is an airfoil from the NACA five digit series, which have the same thickness distributions as their predecessors, the four digit series airfoils, but a maximum camber slightly forward of the mid-chord. Results from the four digit series indicated that the lift coefficient increased as the position of the maximum camber was shifted forward of the mid-chord position. Because the mean camber line of the four digit airfoils was not easily adaptable to the forward position, the five digit series was created with this modification [5].

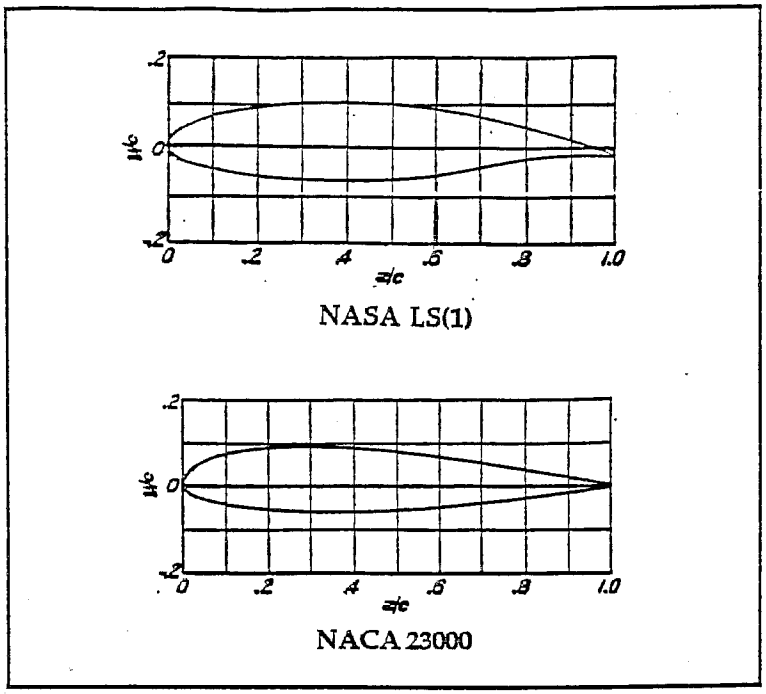

Figure 5.1. Common Wind Turbine Airfoils.

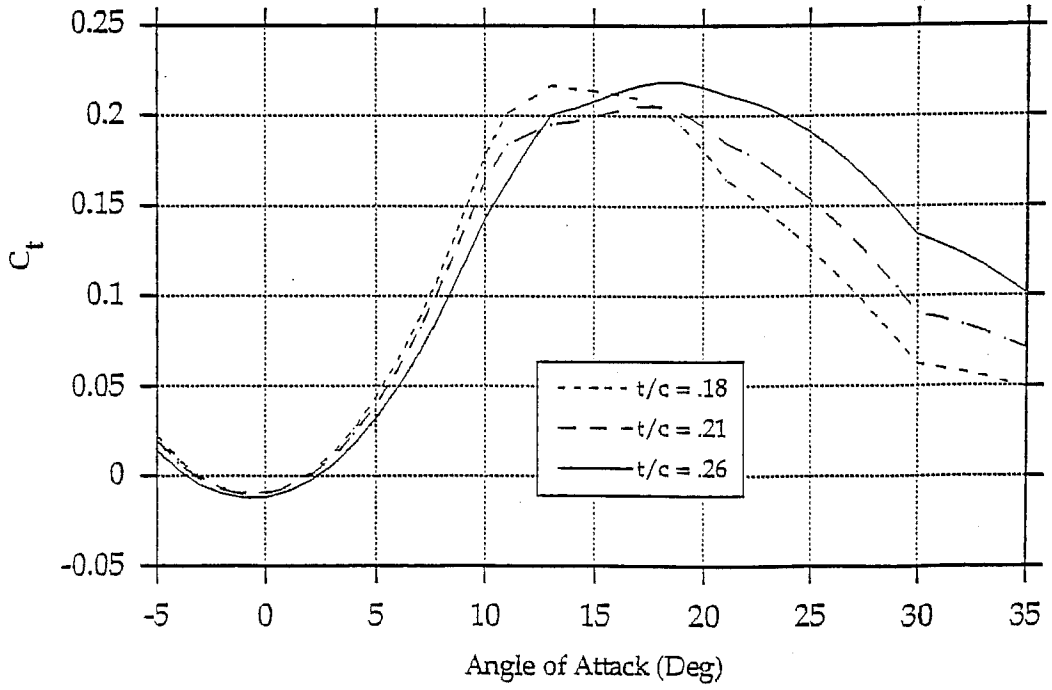

Figure 5.2. LS(1) Tangential Lift Coefficient and Angle of Attack.

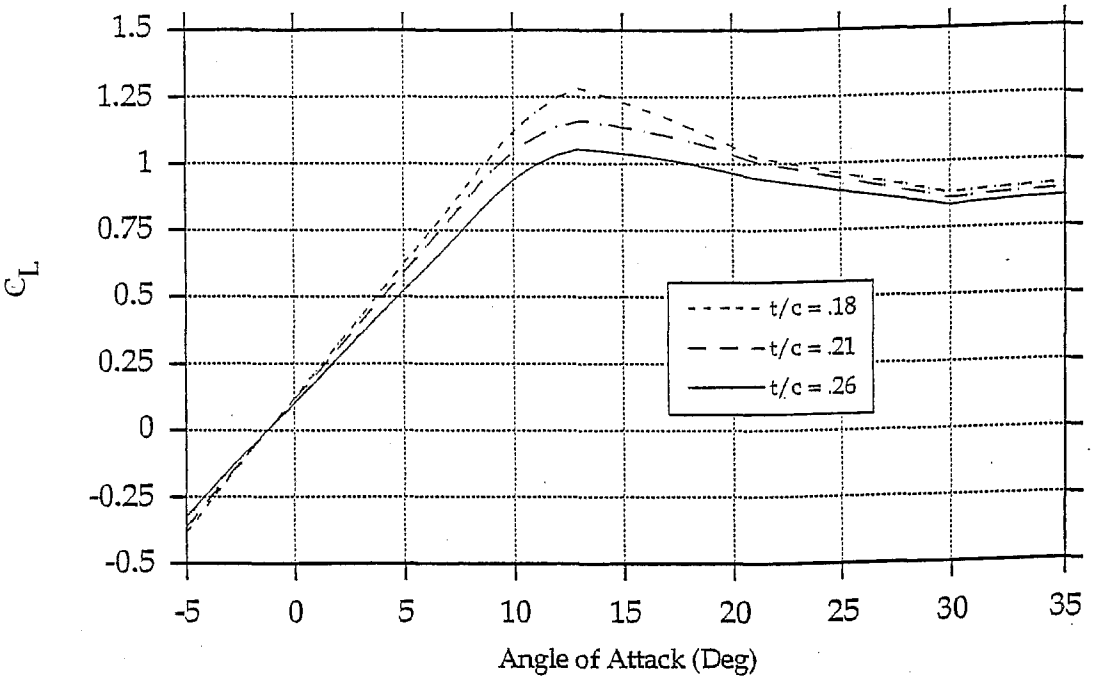

Figure 5.3. LS(1) Lift Coefficient and Angle of Attack.

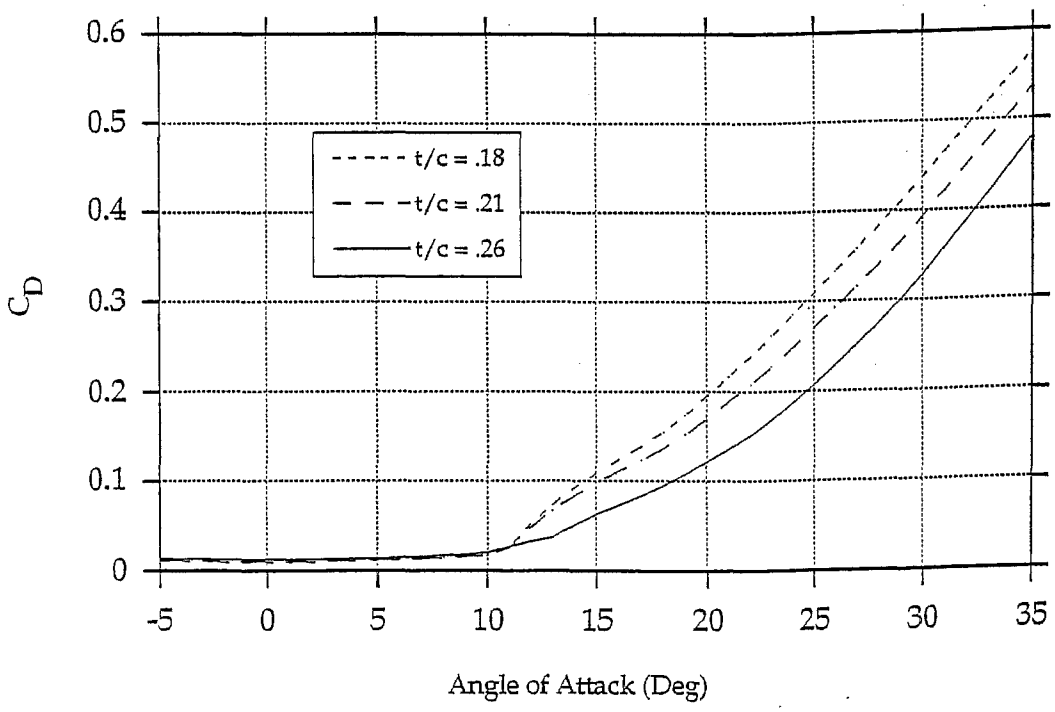

Figure 5.4. LS(1) Drag Coefficient and Angle of Attack.

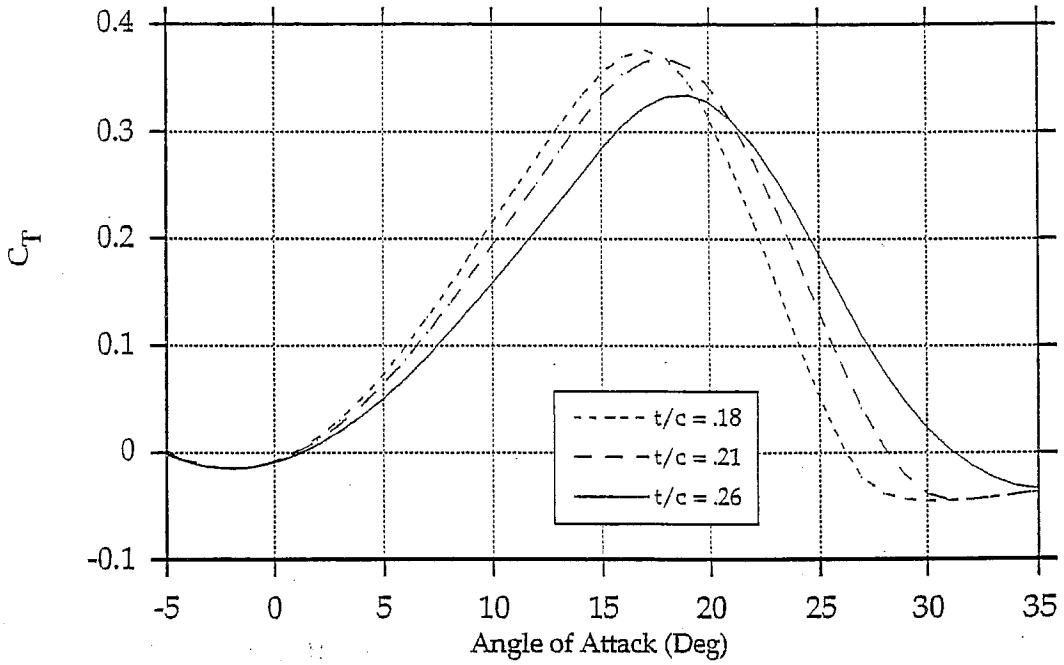

Figure 5.5. NACA 23000 ~~Tangential Lift~~ Coefficient and Angle of Attack.

Chordwise Force

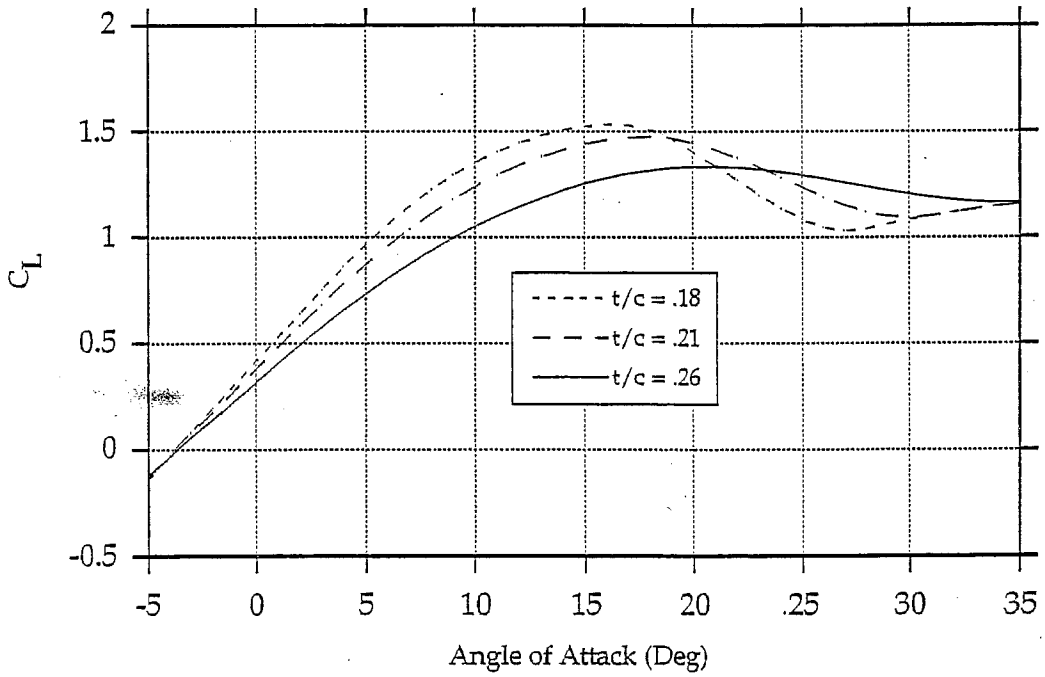

Figure 5.6. NACA 23000 Lift Coefficient and Angle of Attack.

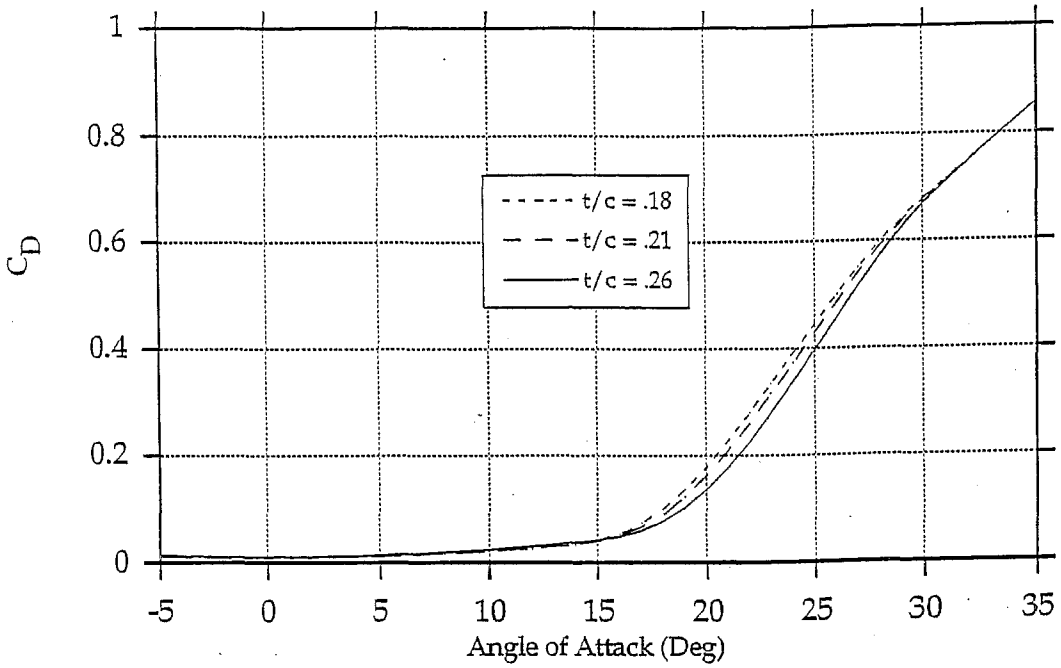

Figure 5.7. NACA 23000 Drag Coefficient and Angle of Attack.

6.0 Subroutine Check

The purpose of subroutine Check is to determine the static deflection of the blade tip and its frequency about this deflection. This is illustrated in Figure 6.1. Calculations for these quantities are based on the first flatwise bending mode of the blade, similar to that of a cantilevered beam. It therefore follows that as the wind speed increases, the static displacement will increase, because the momentum of the wind increases. The tip frequency will, however, stay the same.

Subroutine Check uses the stiffness and mass per unit length tabular data from the input file to determine its outputs-the tip displacement with units of inches and the frequency with units of Hertz. The subroutine does not supply any information to the main program to aid in the prediction of power. Its calculations are performed after the power has been determined.

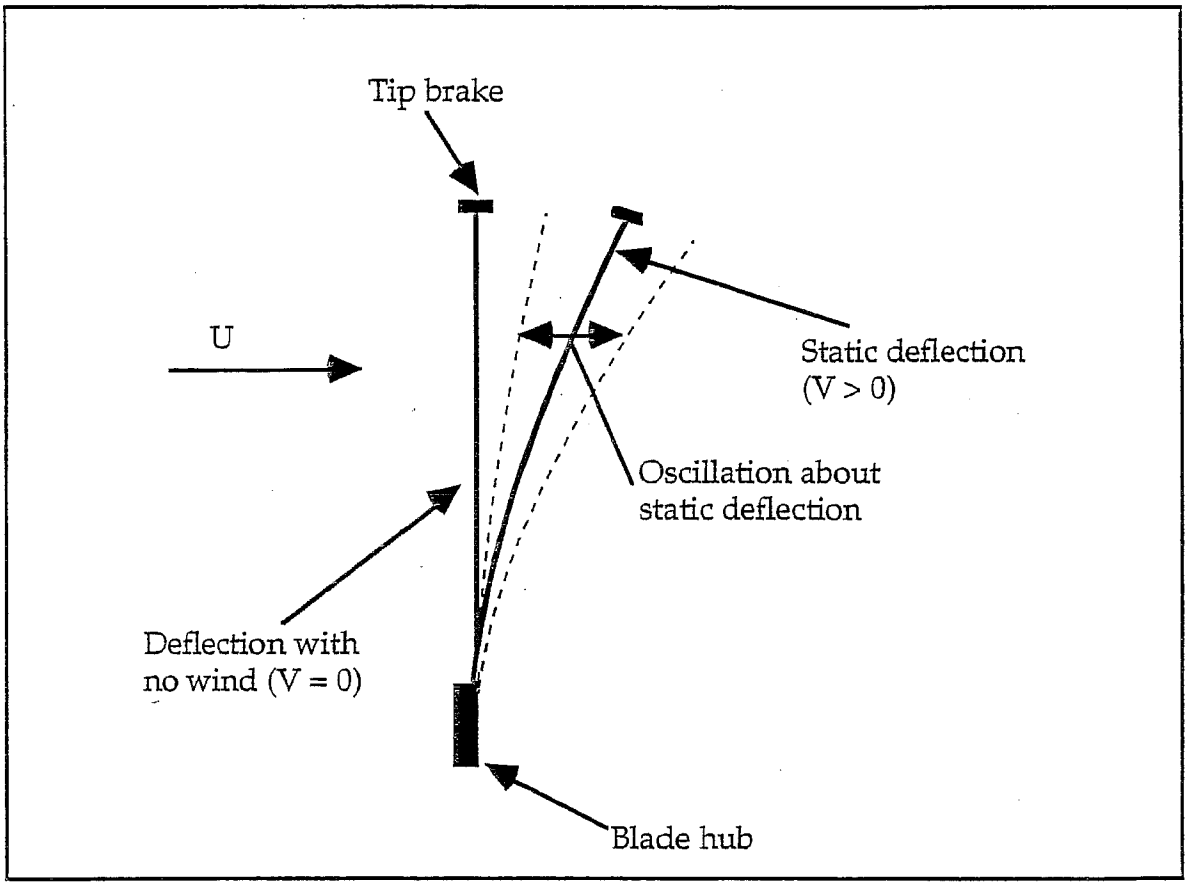

Figure 6.1. Illustration of Static Displacement of First Bending Mode of Single Turbine Blade.

6.1 Derivation of Tip Frequency

The forces acting on a blade element for the first bending mode are shown in Figure 6.2. The tip frequency can be determined by summing forces and moments on the blade element. Summing forces in the u direction gives

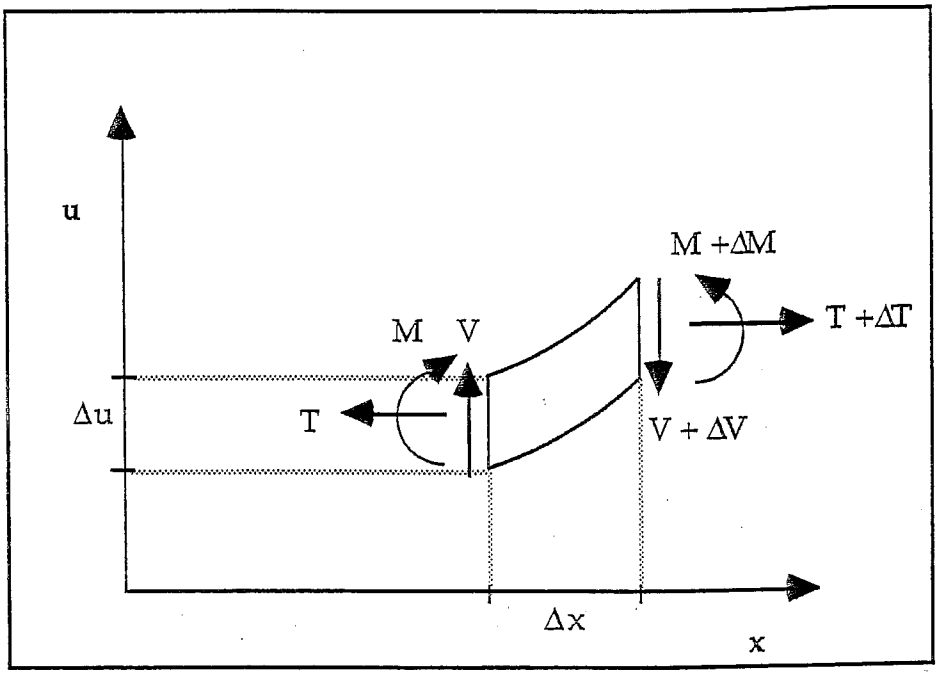

Figure 6.2. Forces and Moments Acting on Blade Element.

$$\sum F_u = V - (V + \Delta V) = \mu \Delta x \frac{\partial^2 u}{\partial t^2}$$

where

μ = mass per unit length

$\mu \Delta x$ = mass of element

This reduces to

$$\frac{\partial V}{\partial x} = -\mu \frac{\partial^2 u}{\partial t^2} \qquad (6.1)$$

Summing the moments about the bottom right corner of the element gives

$$\sum M = (M + \Delta M) - M - \frac{\Delta u}{2}(T + \Delta T) - \frac{\Delta u}{2} T - V \Delta x = 0$$

which reduces to

$$V = \frac{\partial M}{\partial x} - T\frac{\partial u}{\partial x} \tag{6.2}$$

Equation (6.2) can be inserted into (6.1) to give

$$\frac{\partial}{\partial x}\left(\frac{\partial M}{\partial x} - T\frac{\partial u}{\partial x}\right) = -\mu\frac{\partial^2 u}{\partial t^2}$$

From elementary beam theory, the bending moment and shear force are related to the transverse displacement by

$$M = EI\frac{\partial^2 u}{\partial x^2}$$

Inserting this into (6.3) gives

$$\frac{\partial}{\partial x}\left[\frac{\partial}{\partial x}\left(EI\frac{\partial^2 u}{\partial x^2}\right) - T\frac{\partial u}{\partial x}\right] = -\mu\frac{\partial^2 u}{\partial t^2}$$

or

$$\frac{\partial^2(EI)}{\partial x^2}\frac{\partial^4 u}{\partial x^4} - \frac{\partial T}{\partial x}\frac{\partial^2 u}{\partial x^2} + \mu\frac{\partial^2 u}{\partial t^2} = 0 \quad \text{or} \quad EIu_{xx})_{xx} - Tu_x)_x + \mu u_{tt} = 0 \tag{6.4}$$

The displacement in the u direction can be broken into a mode shape and a time dependent function. This can be written as

$$u(x,t) = \phi(x)q(t)$$

When this is substituted into (6.4)

$$EI\phi_{xx})_{xx} q - T\phi_x)_x q + \mu\phi q_{tt} = 0$$

Because the solution of q(t) is known to be

$$q(t) = q_{tip}\sin\omega t$$

This can be substituted into the previous equation to become

$$EI\phi_{xx})_{xx} - T\phi_x)_x - \mu\phi\omega^2 = 0$$

If the above is multiplied by $\phi\, dx$, the equation will be in a form that will allow integration by parts.

$$\omega^2 \int_{hub}^{tip} \mu\phi^2 dx = \int_{tip}^{hub} (EI\phi'')''\phi dx - \int_{tip}^{hub} (T\phi')'\phi dx \qquad (6.5)$$

$$\Uparrow \qquad\qquad \Uparrow$$

$$1 \qquad\qquad 2$$

Evaluation of term 1 by integration by parts (twice) results in

$$\int_h^t (EI\phi'')''\phi dx = \phi(EI\phi'')'\Big|_h^t - \int_h^t (EI\phi'')'\phi' dx = \phi(EI\phi'')'\Big|_h^t - EI\phi''\phi'\Big|_h^t + \int_t^h EI\phi''^2 dx$$

because $\phi_{hub} = 0$, $\phi_{tip} = 1$, and there can be no moments at the tip, the above reduces to

$$\int_h^t (EI\phi'')''\phi dx = (EI\phi'')'\Big|_t + \int_t^h EI\phi''^2 dx \qquad (6.6)$$

Because the tip brakes represent an extra mass at the tip of the blade, special consideration must be given to this area. Figure 6.3 shows the forces acting on the brakes. By summing the forces in the u direction, an expression for $(EI\phi'')'$ at the tip can be determined.

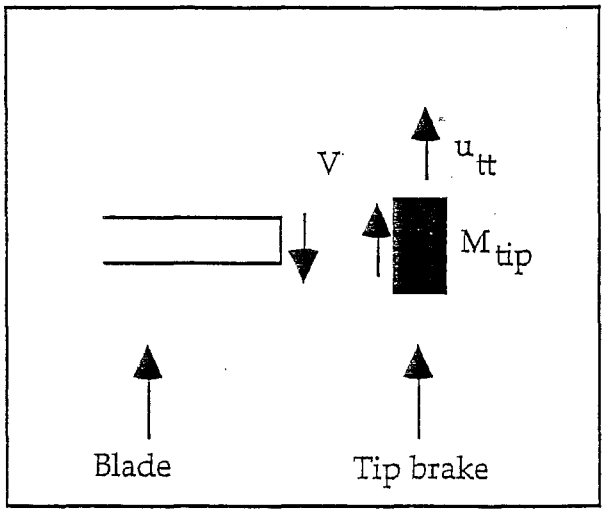

Figure 6.3. End Conditions For Turbine Blade.

From equation (6.2)

$$V = \frac{\partial M}{\partial x} - T\frac{\partial u}{\partial x} \quad \text{or in subscript notation: } V = (EIu_{xx})_x - Tu_x \qquad (6.7)$$

If the vertical forces are summed in Figure 6.3 and equated to (6.7)

$$(EIu_{xx})_x\big|_{tip} - (Tu_x)\big|_{tip} = M_{tip}u_{tt}\big|_{tip}$$

or

$$(EI\phi'')'\big|_{tip} - (T\phi')\big|_{tip} = -M_{tip}\omega^2\phi_{tip} \tag{6.8}$$

Because $\phi_{tip} = 1$, equation (6.8) can be rearranged and inserted into (6.6) to give

$$\int_h^t (EI\phi'')''\phi dx = (T\phi')\big|_{tip} - M_{tip}\omega^2 + \int_t^h EI\phi''^2\,dx \tag{6.9}$$

Evaluation of term 2 in equation (6.5) by integration by parts gives

$$\int_t^h (T\phi')'\phi dx = \phi(T\phi')\Big|_t^h - \int_t^h T\phi'^2\,dx = T\phi\phi'\Big|_t - \int_t^h T\phi'^2\,dx$$

But, because $\phi_{tip} = 1$

$$-\int_t^h (T\phi')'\phi dx = -T\phi'_{tip} + \int_t^h T\phi'^2\,dx \tag{6.10}$$

Inserting (6.9) and (6.10) into (6.5) results in

$$\omega^2 \int_{hub}^{tip} \mu\phi^2 dx = -M_{tip}\omega^2 + \int_t^h EI\phi''^2\,dx + \int_t^h T\phi'^2\,dx$$

Solving for the frequency gives

$$\omega^2 = \frac{\int_h^t EI\phi''^2\,dx + \int_t^h T\phi'^2\,dx}{M_{tip} + \int_h^t \mu\phi^2 dx} \tag{6.11}$$

Equation (6.11) is used by subroutine Check to determine the frequency of the tip. The tension in the blade, T, has yet to be solved for and can be done by summing the forces in the x direction of the blade element in Figure 6.4.

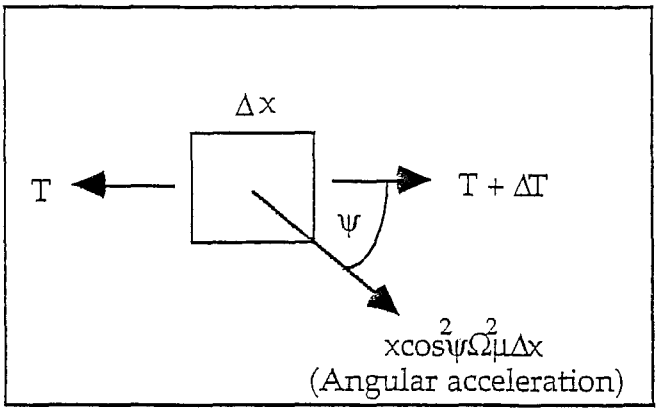

Figure 6.4. Determination of Tension Force in Blade element.

The sum of the forces in the x direction in Figure 6.4 are

$$\sum F_x = T - (T + \Delta T) = \mu\Omega^2 x \cos^2\psi \Delta x$$

or

$$\frac{\partial T}{\partial x} = -\mu\Omega^2 x \cos^2\psi$$

After integrating and applying boundary condition at r=R, the final answer becomes

$$T = R\Omega^2 \cos^2\psi M_{tip} + \Omega^2 \cos^2\psi \int_x^t x\mu dx \qquad (6.12)$$

With the tension in the blade element now known, equation (6.12) can be used in equation (6.11) to determine the blade tip frequency.

6.2 Blade Static Tip Displacement

A similar derivation for the static tip displacement of the blade tip can be derived as for the frequency. This derivation is skipped in the interest of brevity and final equation used by PROPX is given as

$$x_{Tip} = \frac{F_{Blade} - F_{Cent}}{\int_h^t EI\phi''^2 dx + \int_h^t T\phi'^2 dx} \qquad (6.13)$$

where

$$F_{Blade} = \frac{1}{2}\rho V^2 \pi R^2$$

$$F_{Cent} = \sin\psi\cos\psi\left(M_{Tip} R\Omega^2 + \int_h^t \mu\phi x dx \right)$$

6.3 PROPX Implementation

The first part of subroutine Check (flow chart shown in Figure 6.5) involves initializing constants and zeroing variables. The non-dimensionalized length of the blade is calculated based on the distance from the hub to tip, and the tension in the blade at the tip is calculated based on the rotational acceleration and mass of the tip brake. These are given by

$$z = \frac{R_{tip} - R_{hub}}{R_{tip}}$$

$$T_{tip} = R_{tip} M_{tip} \Omega^2$$

The next part of the subroutine involves the integration loop. Each of the four quantities in equation (6.11) are integrated over the non-dimensionalized length of the blade with the simple Rectangular Area method illustrated in Figure 6.6. The integration takes place from the tip of the blade to the hub and can be expressed as the sum of the rectangular areas over the interval from a to b with an incrementation of dx.

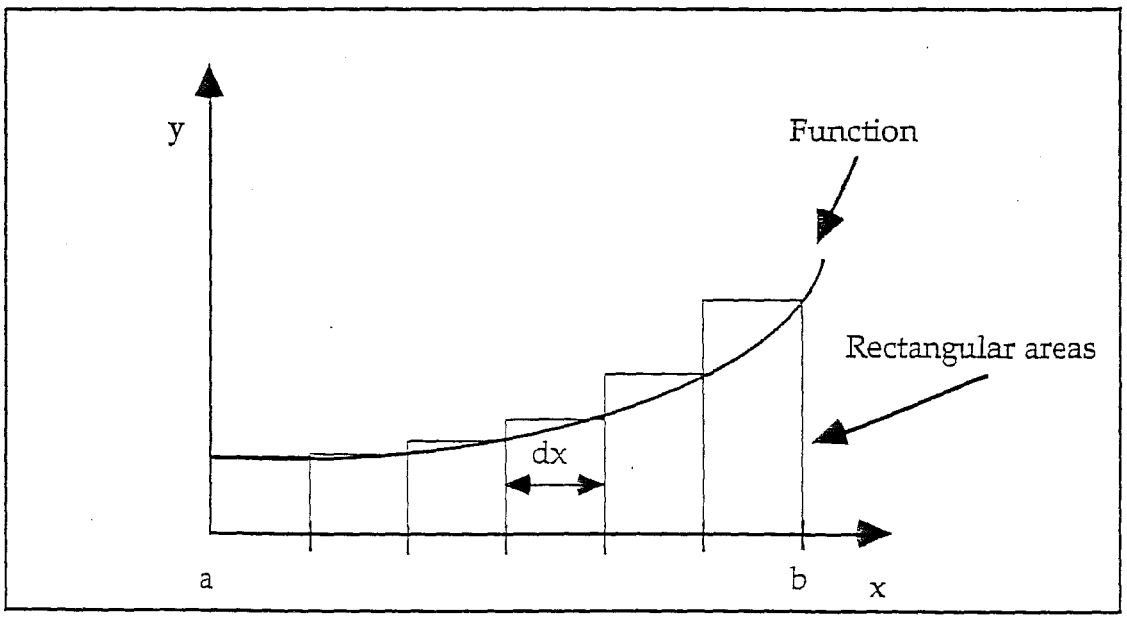

Figure 6.6. Illustration of Rectangular Area Integration Method.

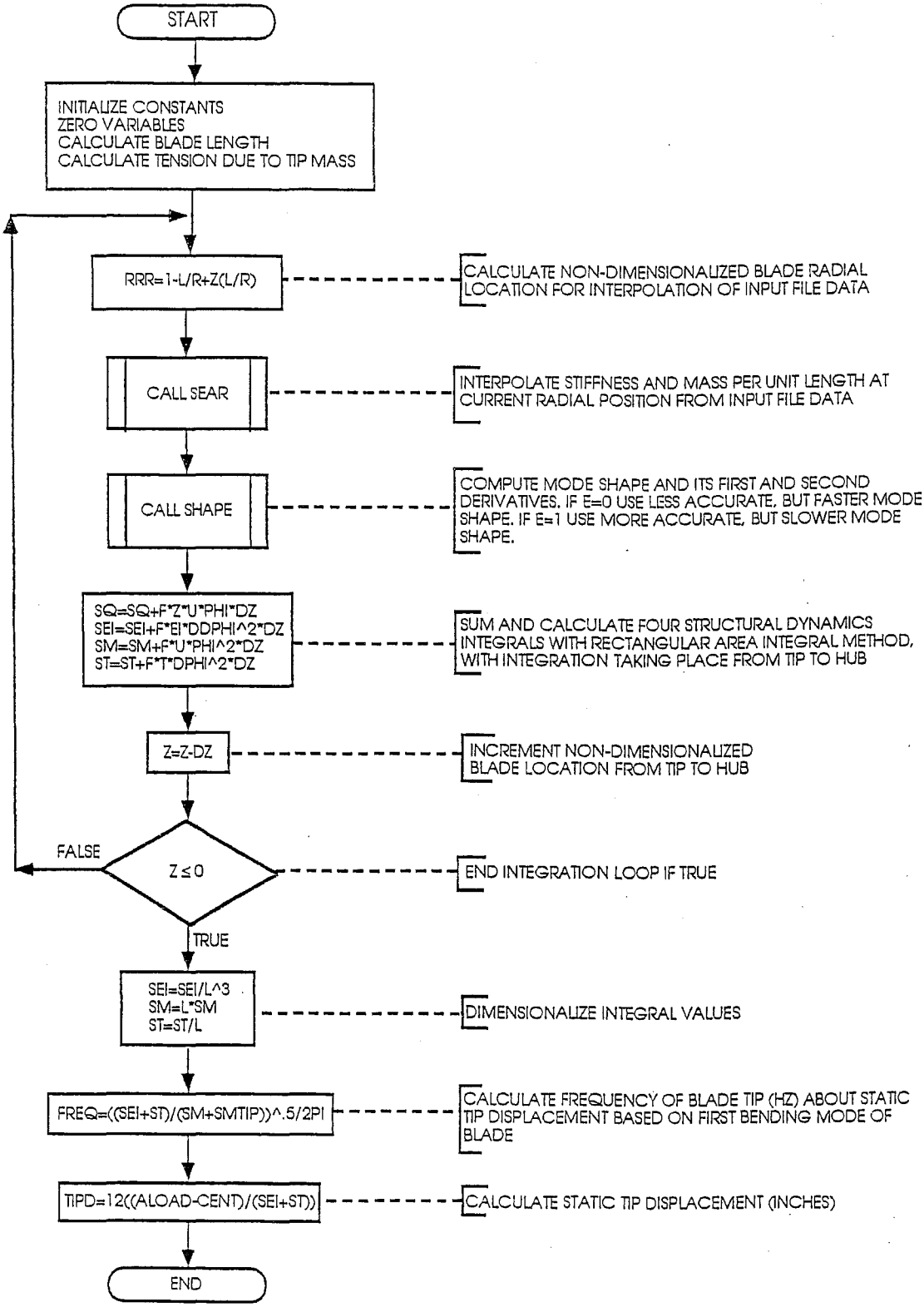

Figure 6.5. Subroutine Check Flow Chart.

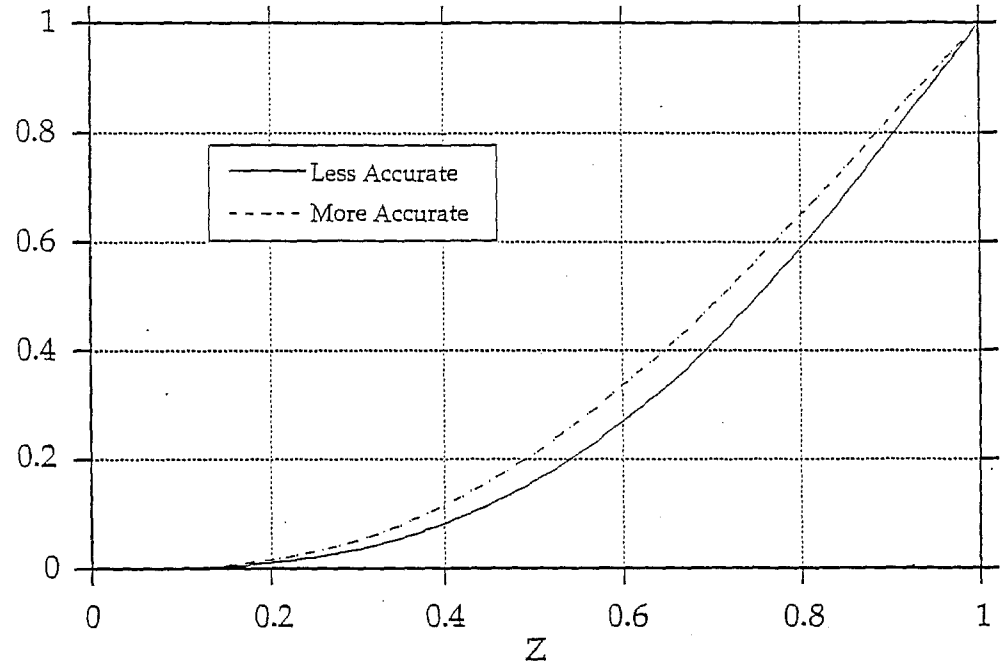

Figure 6.7. Mode Shapes.

s can be written as

$$\int_a^b f(x)dx = \sum f(x)dx$$

s integration method is less accurate than the Simpson's Rule algorithm. The pur-
e of subroutine Check is to give a rough estimate of the frequency and tip displace-
it without slowing the program significantly, so the loss in accuracy is aceptable.

During the integration process, the mode shape, ϕ, also has to be evaluated. In routine Check there is a choice of two mode shape functions. The difference between two being the desired accuracy. Each are shown in Figure 6.7. The most accurate le shape, but slower computationally is given by

$$\phi(z) = \frac{1}{6} z^{3.3}(7.59z^2 - 24.38z - 22.79) \qquad (6.14)$$

re z is the non-dimensionalized length along the blade.

faster, but less accurate mode shape is given by

$$\phi(z) = \frac{1}{2} z^{3.3}(4.3 - 2.3z) \qquad (6.15)$$

The "switch" to incorporate one of the two mode shapes lies in the variable "E" in subroutine Check. If equation (6.14) is desired "E" should be set to 1. If equation (6.15) is desired, "E" should be set to 0. Note that this variable is not in the input file and changing it requires recompilation of the program.

6.4 Final Calculations

Once the mode shape and integrals have been found, they are re-dimensionalized and the tip displacement and frequency are calculated with equations (6.11) and (6.12).

Bibliography

1. Anderson, J. D., Fundamentals of aerodynamics, McGraw-Hill Book Company, New York, 1992.

2. Burden, R. L., and Faires, J. D., Numerical Analysis, PWS Publishers, Boston, 1985.

3. Wilson, R. E., and Walker S. N., Performance Analysis of Horizontal Axis Wind Turbines, NASA Report NAG-3-278, Corvallis, OR, 1984.

4. Wilson, R. E., and Lissaman, B. S., Aerodynamic Performance of Wind Turbines, Oregon State University, Corvallis, OR, 1976.

5. Abbott, I. H., and A. E. von Doenhoff, Theory of Wing Sections, McGraw-Hill Book Company, New York, 1959.

Figure A.1. Input file TEST.INP

```
PERFORMANCE DATA****************************************************
                                                    (Blank Line - Do not delete)
43.0      | ROTOR RADIUS (FT)
0.02      | ROTOR INCREMENT (dr/R)
1.75      | HUB RADIUS (FT)
2.0       | NUMBER OF BLADES
80.0      | HEIGHT OF ROTOR HUB (FT)
0.04      | LOCATION OF GAP (FT)
15.0      | MINIMUM VELOCITY (FT/SEC)
55.0      | MAXIMUM VELOCITY (FT/SEC)
5.0       | VELOCITY INCREMENT (FT/SEC)
7.0       | CONING ANGLE (DEG)
 1.27     | PITCH ANGLE (DEG)
58.0      | ROTATION RATE (RPM)
0.1       | EXPONENT FOR HEIGHT
0.0       | GAP WIDTH (IN)
0.24      | FIXED LOSS FRACTION
0.97      | GEAR BOX EFFICIENCY
0.9539    | GENERATOR EFFICIENCY
300.0     | RATED POWER (KW)
60.0      | TEMPERATURE (DEG F)
860.0     | PRESSURE (MILLIBARS)
0.76      | BENDING MOMENT AT 1ST POSITION (r/R)
0.52      | BENDING MOMENT AT 2ND POSITION (r/R)
0.04      | BENDING MOMENT AT 3RD POSITION (r/R)
21.0      | NUMBER OF INPUT STATIONS FOR BLADE DATA
11.0      | NUMBER OF INPUT STATIONS FOR ELASTIC DATA0
0.0       | NUMBER OF INPUT STATIONS FOR AIRFOIL DATA FILE
6666.0    | AIRFOIL CODE
1.0       | FLAG FOR TANGENTIAL INDUCTION (1-YES 0-NO)
0.08      | FLAT PLATE AREA (FT^2)8
0.777     | TIP MASS (SLUGS)
1.0       | FLAG FOR EXPANDED OUTPUT (1-YES 0-NO)   (Blank Line - Do not delete)
BLADE DATA**********************************************************
                                                    (Blank Line - Do not delete)
LOC(%) CHORD(FT) THETA(DEG) THICKNESS/CHORD
 4.00    2.538     6.10        0.583
 7.60    2.764     5.85        0.583
10.00    2.925     5.69        0.583
15.00    3.238     5.39        0.400
20.00    3.508     5.12        0.347
25.00    3.702     4.83        0.307
30.00    3.792     4.47        0.280
35.00    3.748     4.01        0.260
40.00    3.630     3.45        0.255
45.00    3.511     2.88        0.245
50.00    3.386     2.31        0.236
55.00    3.252     1.76        0.229
60.00    3.108     1.26        0.222
65.00    2.948     0.82        0.215
70.00    2.772     0.48        0.201
75.00    2.577     0.25        0.191
80.00    2.368     0.13        0.187
85.00    2.149     0.08        0.180
90.00    1.917     0.05        0.180
95.00    1.594     0.03        0.180
100.0    1.213     0.00        0.180

ELASTIC DATA********************************************************
                                                    (Blank Line - Do not delete)
LOC(%)  EI(FT^2-LB)  dM/dR(SLUGS/FT)
4.000   104861111.0     2.038
9.900   100972222.0     2.122
13.20   48826333.00     1.021
15.00   43423444.00     1.050
25.00   28326555.00     1.104
45.00   11777666.00     0.810
65.00   4348777.000     0.550
75.00   2268888.000     0.456
85.00   966999.0000     0.351
95.00   249000.0000     0.203
100.0   248111.0000     0.203
```

A.2 Explanation of Inputs

Some of the inputs to the input file are not as obvious as others, so a brief description of each is given below.

Rotor radius-The distance from the center of the turbine to the tip of the blade.

Rotor increment-This is used to establish the number of intervals along the blade (the size of dr). The increment can be calculated with

$$\text{Rotor Increment} = \frac{R_{Tip} - R_{Hub}}{NR_{Tip}}$$

where N is the number of sections in which the blade is to be discretized. Twenty is usually a good compromise between speed and accuracy.

Hub radius-The distance from the center of the turbine to the beginning of the blade.

Number of blades-Self explanatory.

Height of rotor hub-The vertical distance from the ground center of the rotor.

Location of gap-The distance from the center of the turbine to a gap in the rotor blade. This is usually associated with aerodynamic control devices. In the case of the ESI-80, this was set to a location not on the blade, because there are no gaps.

Maximum/Minimum velocity-The highest and lowest wind speeds for the turbine operating conditions.

Velocity increment-The change in velocity from the minimum to maximum velocity.

Coning Angle-The tilt angle of the blade to relieve shaft stresses.

Pitch angle-The angle about which the entire blade is rotated.

Rotation rate-The rotations per minute of the blade.

Exponent for height-This describes the roughness of the terrain surrounding the turbine. This value is usually between 0.1 and 0.2.

Gap width-The width of space in the blade caused by aerodynamic control mechanisms. In this case there are none.

Fixed loss fraction-The losses in the generator caused by the field, windage, and current losses. This is usually between 1/3 and 1/2.

Gear box/Generator efficiencies-Self explanatory.

Rated Power-The maximum allowable power for normal every day operation.

Temperature/Pressure-The ambient temperature and pressure.

Bending moment-There are three locations along the blade in which bending moments can be determined.

Number of input stations for blade/elastic data-The number of rows of data for the blade or elastic data.

Number of input stations for airfoil data-The number of rows of airfoil data to be read in from separate file. This line is not necessary if the built in airfoil subroutines are used.

Airfoil code-The number code for the desired airfoil-7777 for LS(1), 8888 for data file input characteristics, 9999 for NACA 23000.

Flag for tangential induction-When turned on, this includes the effects of a rotating wake.

Flat plate area-The frontal area of the tip brake for slowing turbine in excessive winds.

Tip mass-The mass of the tip brake.

Flag for expanded output-This controls the detail of the output file. See Appendix B.

Tabular data sections:

Loc-The percent location along the blade of each of the following parameters.

Chord-The length of the airfoil section from the leading edge to trailing edge.

Theta-The twist angle.

Thickness/Chord-The maximum thickness of the airfoil divided by the chord length.

EI-Blade stiffness parameter used in subroutine Check.

dM/dR-The mass per unit length of blade section used in subroutine Check.

Appendix B: Propx Output File

The output for the input file in Appendix A is shown on the next page in expanded format. It contains output only for the first two wind speeds (13 and 15 MPH) in order to save space. The output for the remaining wind speeds looks the same except that the predicted power increases with wind speed.

The beginning of the output file contains most of the operating conditions given in the input file. This section usually takes up the first page of the output and is printed only once.

The remainder of the output details the performance characteristics calculated by PROPX. This output is repeated once for every incrementation in wind speed. The length of this part of the output can be considerably long, so it is sometimes desirable to shorten the format in the input file.

The unexpanded output format is the same as the expanded, except that none of the values in the Performance Analysis section of the output are printed. Values given in the expanded output include, respectively: blade non-dimensionalized location, axial induction factor, tangential induction factor, lift coefficient, drag coefficient, relative inflow angle, angle of attack, change in angle of attack due to cascade effects, tangential force, Reynold's Number, and the number of iterations necessary for the axial induction factor to converge. The expanded output can be "turned off" in the input file.

THEORETICAL PERFORMANCE OF A PROPELLER TYPE WIND TURBINE

OPERATING CONDITIONS:

WIND SPEED GRADIENT EXPONENT = .1000
HUB HEIGHT ABOVE GROUND LEVEL - FT- = 80.0000
AIR TEMPERATURE - DEGREES F = 60.0000
BAROMETRIC PRESSURE - MB = 860.0000
ANGULAR VELOCITY - RADIAN PER SEC = 6.0737
PITCH ANGLE FROM NOMINAL TWIST - DEGREES = 1.2700
PITCH ANGLE AT 0.75 RADIUS - DEGREES = 1.5065
CONING ANGLE - DEGREES = 7.0000

DRIVE TRAIN:

GENERATOR RATING--KW = 300.0
MAX GENERATOR EFFICIENCY = .9539
GENERATOR FIXED LOSS FRACTION = .2400
GEAR BOX EFFICIENCY = .9700

BLADE DESIGN:

NUMBER OF BLADES = 2.
TIP RADIUS - FT = 43.0000
HUB RADIUS - FT = 1.7500
SOLIDITY = .04186
NUMBER OF STATIONS ALONG SPAN = 21
GAP WIDTH - INCHES = .0000
GAP AT RADIUS RATIO = .0400

CHORD, TWIST DISTRIBUTION, AND THICKNESS

PERCENT RADIUS	CHORD-FT	TWIST-DEG	THICK/CHORD
4.00	2.53800	6.10000	.58300
7.60	2.76400	5.85000	.58300
10.00	2.92500	5.69000	.58300
15.00	3.23800	5.39000	.40000
20.00	3.50800	5.12000	.34700
25.00	3.70200	4.83000	.30700
30.00	3.79200	4.47000	.28000
35.00	3.74800	4.01000	.26000
40.00	3.63000	3.45000	.25500
45.00	3.51100	2.88000	.24500
50.00	3.38600	2.31000	.23600
55.00	3.25200	1.76000	.22900
60.00	3.10800	1.26000	.22200
65.00	2.94800	.82000	.21500
70.00	2.77200	.48000	.20100
75.00	2.57700	.25000	.19100
80.00	2.36800	.13000	.18700
85.00	2.14900	.08000	.18000
90.00	1.91700	.05000	.18000
95.00	1.59400	.03000	.18000
100.00	1.21300	.00000	.18000

PROGRAM OPERATING CONDITIONS:

CALCULATIONS INCLUDE TANGENTIAL INDUCTION
WIND TURBINE AIRFOIL CURVEFIT AERODYNAMICS -- 6666
INCREMENTAL PERCENTAGE = .0200
1ST ORDER MOMENTUM CORRECTION
TIP LOSSES MODELED BY PRANDTLS FORMULA
NO HUBLOSS MODEL USED

PERFORMANCE ANALYSIS:

PCCR	A	AP	CL	CD	PHI	ALPHA	DALPHA	dFt/dr	RENO	ITER
.980	.3824	.0018	.383	.0061	3.03	1.82	.07	1.27	.187E+07	4
.960	.3346	.0017	.416	.0061	3.34	2.12	.08	1.73	.204E+07	4
.940	.3196	.0018	.432	.0062	3.48	2.27	.09	2.01	.219E+07	3
.920	.3157	.0018	.443	.0062	3.58	2.36	.10	2.22	.231E+07	2
.900	.3180	.0019	.451	.0062	3.65	2.43	.11	2.39	.242E+07	3
.880	.3192	.0020	.459	.0062	3.72	2.51	.12	2.51	.248E+07	2
.860	.3230	.0021	.466	.0062	3.79	2.57	.12	2.61	.254E+07	3
.840	.3274	.0022	.471	.0062	3.85	2.62	.13	2.69	.258E+07	3
.820	.3319	.0024	.476	.0063	3.92	2.68	.14	2.75	.262E+07	3
.800	.3372	.0025	.480	.0064	3.98	2.74	.16	2.80	.266E+07	3
.780	.3413	.0027	.483	.0064	4.06	2.78	.17	2.84	.268E+07	3
.760	.3458	.0028	.487	.0064	4.14	2.82	.18	2.88	.271E+07	3
.740	.3487	.0030	.490	.0065	4.23	2.85	.19	2.91	.272E+07	2
.720	.3501	.0032	.491	.0066	4.34	2.89	.21	2.93	.273E+07	2
.700	.3518	.0033	.494	.0066	4.45	2.92	.22	2.95	.273E+07	2
.680	.3506	.0035	.494	.0067	4.58	2.94	.24	2.96	.272E+07	2
.660	.3502	.0037	.496	.0069	4.72	2.97	.26	2.97	.270E+07	1
.640	.3503	.0040	.500	.0069	4.87	2.97	.28	2.98	.268E+07	2
.620	.3497	.0042	.505	.0070	5.03	2.98	.30	3.00	.266E+07	1
.600	.3502	.0045	.512	.0070	5.19	2.99	.32	3.03	.263E+07	1
.580	.3500	.0048	.519	.0071	5.37	2.98	.34	3.05	.259E+07	1
.560	.3509	.0052	.528	.0071	5.55	2.99	.37	3.07	.255E+07	2
.540	.3522	.0056	.540	.0072	5.74	2.99	.39	3.10	.250E+07	2
.520	.3539	.0061	.553	.0072	5.94	3.00	.42	3.12	.245E+07	2
.500	.3565	.0066	.569	.0073	6.15	3.01	.44	3.15	.239E+07	2
.480	.3616	.0072	.590	.0074	6.35	3.02	.48	3.19	.233E+07	2
.460	.3678	.0079	.615	.0074	6.56	3.03	.51	3.23	.227E+07	2
.440	.3757	.0087	.644	.0075	6.76	3.04	.55	3.27	.221E+07	3
.420	.3853	.0096	.678	.0076	6.96	3.06	.59	3.31	.214E+07	3
.400	.3958	.0107	.717	.0076	7.18	3.09	.63	3.35	.207E+07	3
.380	.4002	.0118	.750	.0077	7.49	3.22	.68	3.38	.199E+07	2
.360	.4050	.0132	.787	.0078	7.83	3.38	.72	3.40	.191E+07	2
.340	.4204	.0150	.850	.0079	8.05	3.47	.78	3.44	.183E+07	3
.320	.4474	.0171	.944	.0080	8.14	3.45	.86	3.48	.173E+07	3
.300	.4757	.0196	1.052	.0082	8.22	3.42	.94	3.49	.164E+07	3
.280	.4683	.0224	1.114	.0083	8.89	4.04	1.03	3.50	.152E+07	2
.260	.4615	.0258	1.186	.0085	9.65	4.75	1.12	3.51	.141E+07	2
.240	.4543	.0301	1.273	.0088	10.53	5.60	1.23	3.52	.129E+07	2
.220	.4464	.0355	1.378	.0092	11.57	6.64	1.35	3.51	.116E+07	2
.200	.4391	.0425	1.500	.0097	12.77	7.86	1.48	3.50	.105E+07	2
.180	.4305	.0518	1.651	.0105	14.23	9.35	1.62	3.47	.927E+06	2
.160	.4205	.0644	1.820	.0117	16.00	11.17	1.77	3.43	.814E+06	2
.140	.3987	.0815	1.966	.0215	18.50	13.84	2.06	3.31	.708E+06	4
.120	.3544	.1037	2.024	.0804	22.32	17.96	2.49	2.94	.610E+06	7
.100	.2986	.1331	1.998	.2765	27.53	23.46	2.89	2.19	.522E+06	8
.080	.1899	.1505	1.615	.6585	36.55	32.16	2.70	1.07	.447E+06	7
.060	.1676	.2274	1.622	.8628	43.60	38.60	2.23	.92	.378E+06	6
.041	.1568	.4083	1.564	1.0523	51.10	44.93	1.19	.80	.324E+06	8

PERFORMANCE SUMMARY: TIP SPEED RATIO = 11.871

WINDSPEED ; MPH= 15.00 M/S= 6.71
IDEAL POWER COEFFICIENT = .44124
GAP CORRECTION DCP = .0000000
CP CORRECTED FOR SHEAR AND GAP = .43822
IDEAL THRUST COEFFICIENT = .9185
AERO BENDING MOMENT (FT-LB) AT 32.4364 RADIUS = 2207.6
AERO BENDING MOMENT (FT-LB) AT 22.1933 RADIUS = 9314.8
AERO BENDING MOMENT (FT-LB) AT 1.7072 RADIUS = 33210.8
FREQ (HZ) = 2.869
TIP DISPLACEMENT (INCHES) = -2.84
ROTOR POWER - KW = 37.1
ELECTRICAL OUTPUT - KW = 32.3

PERFORMANCE ANALYSIS:.

PCCR	A	AP	CL	CD	PHI	ALPHA	DALPHA	dFt/dr	RENO	ITER
.980	.3347	.0030	.528	.0063	4.35	3.13	.07	3.03	.188E+07	6
.960	.2875	.0028	.573	.0064	4.75	3.53	.08	3.94	.205E+07	4
.940	.2705	.0029	.597	.0064	4.97	3.75	.09	4.55	.219E+07	4
.920	.2639	.0029	.614	.0065	5.12	3.90	.09	5.02	.231E+07	3
.900	.2631	.0031	.627	.0065	5.24	4.02	.10	5.42	.243E+07	1
.880	.2617	.0032	.641	.0065	5.37	4.14	.11	5.72	.249E+07	2
.860	.2626	.0033	.653	.0066	5.48	4.26	.12	5.98	.255E+07	2
.840	.2646	.0035	.664	.0066	5.60	4.37	.13	6.20	.259E+07	2
.820	.2672	.0037	.674	.0067	5.71	4.47	.14	6.38	.263E+07	3
.800	.2708	.0039	.683	.0068	5.82	4.57	.15	6.55	.267E+07	3
.780	.2738	.0042	.692	.0068	5.95	4.66	.16	6.68	.270E+07	3
.760	.2774	.0044	.701	.0069	6.07	4.75	.17	6.80	.272E+07	3
.740	.2801	.0047	.708	.0070	6.21	4.83	.18	6.90	.273E+07	2
.720	.2820	.0050	.714	.0071	6.36	4.90	.20	6.98	.274E+07	2
.700	.2842	.0053	.721	.0072	6.52	4.98	.21	7.05	.274E+07	2
.680	.2845	.0056	.727	.0073	6.71	5.05	.23	7.09	.273E+07	1
.660	.2854	.0060	.733	.0074	6.89	5.12	.25	7.12	.272E+07	2
.640	.2866	.0064	.743	.0075	7.09	5.19	.27	7.17	.270E+07	1
.620	.2874	.0068	.752	.0076	7.31	5.24	.29	7.20	.268E+07	2
.600	.2889	.0073	.765	.0076	7.53	5.31	.31	7.25	.265E+07	2
.580	.2899	.0078	.778	.0077	7.77	5.37	.33	7.29	.261E+07	2
.560	.2915	.0084	.795	.0078	8.02	5.44	.35	7.33	.257E+07	2
.540	.2934	.0090	.813	.0079	8.29	5.52	.37	7.37	.252E+07	2
.520	.2955	.0098	.835	.0079	8.57	5.60	.39	7.42	.247E+07	2
.500	.2982	.0106	.859	.0080	8.87	5.70	.42	7.47	.242E+07	2
.480	.3023	.0116	.889	.0081	9.17	5.80	.44	7.52	.236E+07	3
.460	.3072	.0127	.924	.0082	9.48	5.92	.47	7.59	.230E+07	3
.440	.3131	.0140	.964	.0084	9.81	6.05	.50	7.66	.224E+07	3
.420	.3200	.0156	1.011	.0085	10.15	6.20	.54	7.74	.217E+07	3
.400	.3275	.0173	1.063	.0086	10.52	6.37	.58	7.82	.210E+07	3
.380	.3314	.0193	1.109	.0088	10.97	6.64	.61	7.85	.203E+07	3
.360	.3355	.0216	1.161	.0089	11.47	6.95	.65	7.89	.195E+07	3
.340	.3458	.0245	1.241	.0091	11.92	7.24	.69	7.98	.187E+07	3
.320	.3631	.0281	1.356	.0094	12.27	7.47	.75	8.09	.177E+07	3
.300	.3813	.0325	1.486	.0097	12.65	7.72	.81	8.18	.168E+07	3
.280	.3765	.0370	1.569	.0101	13.56	8.55	.87	8.13	.157E+07	2
.260	.3720	.0425	1.664	.0106	14.59	9.49	.93	8.08	.145E+07	2
.240	.3664	.0492	1.774	.0113	15.78	10.61	.99	8.01	.134E+07	2
.220	.3553	.0573	1.882	.0124	17.28	12.06	1.05	7.89	.122E+07	3
.200	.3379	.0671	1.969	.0221	19.21	13.92	1.10	7.61	.111E+07	4
.180	.3090	.0783	2.019	.0520	21.79	16.43	1.14	7.06	.992E+06	6
.160	.2725	.0909	2.018	.1239	25.08	19.63	1.16	6.16	.886E+06	7
.140	.2355	.1063	2.000	.2817	29.00	23.56	1.28	4.88	.785E+06	7
.120	.1638	.1098	1.705	.5836	35.19	29.98	1.63	2.77	.694E+06	13
.100	.1458	.1399	1.722	.7520	40.09	34.98	1.84	2.35	.609E+06	3
.080	.1299	.1900	1.715	.9089	45.75	40.11	1.45	2.09	.532E+06	4
.060	.1173	.2864	1.653	1.0740	52.10	45.67	.80	1.84	.467E+06	7
.041	.1094	.5017	1.496	1.2224	58.58	50.96	-.26	1.51	.416E+06	9

PERFORMANCE SUMMARY: TIP SPEED RATIO = 8.904

WINDSPEED ; MPH= 20.00 M/S= 8.94
IDEAL POWER COEFFICIENT = .45688
GAP CORRECTION DCP = .0000000
CP CORRECTED FOR SHEAR AND GAP = .45419
IDEAL THRUST COEFFICIENT = .7541
AERO BENDING MOMENT (FT-LB) AT 32.4364 RADIUS = 3084.5
AERO BENDING MOMENT (FT-LB) AT 22.1933 RADIUS = 13260.5
AERO BENDING MOMENT (FT-LB) AT 1.7072 RADIUS = 48181.6
FREQ (HZ) = 2.869
TIP DISPLACEMENT (INCHES) = .40
ROTOR POWER - KW = 91.0
ELECTRICAL OUTPUT - KW = 84.0